Magnetic dipole excitations in deformed nuclei

N. Lo Iudice
Dipartimento di Scienze Fisiche, Universitá di Napoli "Federico II" and Istituto Nazionale di Fisica Nucleare, Naples, Italy

Fiz. Élem. Chastits At. Yadra **28**, 1389–1456 (November–December 1997)

The many models adopted to study the properties of the low-lying magnetic dipole excitations known as the scissors mode observed in most deformed nuclei are reviewed. Attention is focused first on the geometrical two-rotor model (TRM), whose predictions gave the motivation for seeking such a mode. The consistency of these predictions with the most meaningful collective properties of the mode is emphasized. More sophisticated descriptions carried out within different boson models are then reviewed. Their strict connection with the TRM is proved. An even closer link is shown to exist between the TRM and the schematic random-phase approximation (RPA). From the phenomenological and schematic models, confined to the description of the collective features of the M1 transitions, the analysis moves to the fully microscopic approaches, the only ones capable of accounting for the global properties of the mode as well as for the fragmentation of its M1 strength. Shell-model approaches, widely adopted for light and medium-light nuclei, are discussed. A more detailed analysis is devoted to the RPA, the most widely adopted microscopic scheme, especially in heavy nuclei. The path leading from the early incomplete and too approximate approaches yielding contradictory results to the most recent and refined studies converging to similar conclusions is sketched. The quasiparticle–phonon model (QPNM) as a way of improving the RPA description of the M1 spectrum by including the coupling to two-phonon RPA states is finally illustrated, and the related results are discussed. The study of the M1 spectra observed recently in deformed odd-mass nuclei carried out in a QPNM context completes the review.
 [S1063-7796(97)00206-4]

1. INTRODUCTION

The field of magnetic dipole response has expanded considerably in scope since the discovery of low-lying M1 excitations, known as the scissors mode, made by Richter and coworkers in ^{156}Gd through a high-resolution inelastic electron scattering experiment.[1] The search for such a mode was stimulated by the prediction, made within the TRM,[2] of a collective M1 mode promoted by a rotational oscillation of proton versus neutron deformed fluids. The name "scissors mode" was indeed suggested by such a geometrical picture. A magnetic excitation of similar nature was predicted as a mixed-symmetry state in the proton–neutron interacting-boson model (IBM2)[3,4] and as a giant angle resonance in a schematic model.[5]

The discovery has led to a renaissance of low-energy nuclear spectroscopy. Not only electron scattering but also nuclear-resonance fluorescence (NRF) and proton scattering have been adopted for a systematic search for this new mode. As summarized in several review articles,[6–10] the mode has been detected in most of the deformed nuclei ranging from the (f,p) shell to the rare-earth and actinide regions. The search has also stimulated important advances in the experimental techniques, which have enabled a quite complete characterization of the mode. It is well established by now that this is fragmented into several closely packed M1 transitions. These are mainly promoted by the convection current, and their summed M1 strength grows quadratically with the nuclear deformation parameter. This latter property was found recently in the rare-earth region[11–15] and represents the most spectacular signature of the mode.

With the use of Compton polarimeters in NRF, which has enabled parity assignment,[16] unexpectedly strong E1 transitions in the same energy range as the scissors mode, or immediately below, have been detected.[17–20]

Another by-product of the systematic study of the mode has been the discovery of spin excitations. Inelastic proton scattering experiments on ^{154}Sm and other deformed nuclei[21] have found a sizable, strongly fragmented M1 spin strength distributed over an energy range of 4 to 12 MeV, so as to give rise to a double hump.[22]

The experimental discovery has stimulated a proliferation of theoretical investigations. The gross features of the mode were analyzed in several phenomenological models. We recall among them the IBM2,[23–29] the extended Bohr–Mottelson model,[30] the closely related neutron–proton deformation model (NPD),[31] and the generalized coherent-state model (CGSM).[32,33] Studies carried out in a sum-rule approach,[34] in a schematic random-phase approximation,[35–37] and in a mean-field context[38] have given illuminating insights into the shell structure of the mode.

Phenomenological and schematic models ignore many degrees of freedom, such as spin. For this reason they are inadequate for describing the detailed structure of the mode. An exhaustive analysis covering also the energy strength distribution can be carried out only in fully microscopic approaches.

Microscopic calculations were performed in the context of the standard shell model for medium-light nuclei.[39–42] These can be viewed as the microscopic counterpart of an extended version of the interacting-boson model, the IBM3, also used to study the M1 mode in the same nuclei.[43,44] An alternative and valid approach for this nuclear region has consisted in adopting an $SU(3)$ shell-model basis.[45–47] The same $SU(3)$ scheme was modified so as to enable the description of the mode also in heavy nuclei.[48,49] In heavy deformed nuclei, however, apart from a few exceptions,[50,51] most of the microscopic studies were carried out in the RPA[52–77] or in the Tamm–Dancoff approximation (TDA).[78,79]

A new boost to theoretical studies has been stimulated by the discovery of the quadratic deformation law. This property has been studied in practically all models adopted previously, either in the microscopic (Refs. 42, 69, 74, 77, and 79–83) or in the phenomenological domain.[79,84–92] All these analyses give conclusive support to the scissors nature of the magnetic transitions found experimentally. Nonetheless, a complete detailed understanding of the related phenomenology is still lacking. The present situation is in fact more complex than that of the E1 resonance. In contrast to the case of the E1 mode, the M1 transitions lead to bound states, so that the theoretical models have to reproduce the pattern of fragmentation instead of a broad peak. Another feature of the M1 mode which complicates its description is, for example, the interplay between spin and orbital motion. Because of the many degrees of freedom involved in the transitions, several components of the nuclear Hamiltonian enter into play in determining the size and the distribution pattern of the strength. All these aspects are taken into account in RPA calculations. These, however, being confined within a space spanned by two-quasiparticle states, may miss some configurations which enter into the M1 channel either directly or through coupling.

An effort for improving and extending the TDA and RPA calculations has been made recently by studying the mode within the quasiparticle–phonon nuclear model (QPNM),[93] which accounts for the coupling to two RPA phonons.[94]

Theoretical studies have also posed the question of whether the scissors mode survives as one moves from even- to odd-mass nuclei.[95–98] After a first negative attempt carried out in electron scattering,[99] NRF experiments have detected in several odd-mass deformed nuclei of the rare-earth region a sizable dipole strength, whose distribution pattern follows closely the M1 spectrum of the nearby even-mass partners.[20,100,101] Schematic and phenomenological models are even more inadequate for facing the extreme complexity of the M1 spectrum in odd-mass nuclei. Fully microscopic calculations are badly needed for this purpose. The first and only calculation of this kind has been carried out recently, using the QPNM formalism.[102,103]

Section 2 deals with the TRM prediction and the experimental evidence for the mode. The systematic experimental analyses are briefly reviewed. The consistency of the model with the deformation law is discussed. Its microscopic formulation is illustrated. In Sec. 3 the description of the mode within different boson models is discussed. The analysis covers the extended Bohr–Mottelson, the NPD, the GCSM, and the algebraic IBM2 models. The review then moves to shell-model studies (Sec. 4). Standard as well as $SU(3)$ shell-model calculations are presented. The microscopic investigations proceed with the RPA. The method, the problems encountered by the early calculations, the way of solving them, and, finally, the most meaningful results are discussed in Sec. 5. We then go beyond the RPA by reviewing briefly the QPNM and by discussing the results obtained in relation to experiments and the RPA (Sec. 6). The review is completed by a discussion of the M1 spectra observed in deformed odd-mass nuclei and studied within the QPNM formalism in Sec. 7. Conclusions are drawn in Sec. 8.

2. SCISSORS MODE: PREDICTION AND EXPERIMENTAL EVIDENCE

The angular momentum carried out by the nucleus does not produce any intrinsic excitation. This reflects the spherical symmetry of the nuclear Hamiltonian, just as its translational invariance forbids the occurrence of an isoscalar collective E1 mode. One may, however, carry further the analogy with translations and assume that protons and neutrons form two distinct deformed fluids free to rotate separately about a common axis (perpendicular to their symmetry axes). Because of their mutual interaction, they may undergo a rotational oscillation giving rise to an intrinsic M1 excitation. This is the underlying idea of the TRM,[2] which represents the rotational counterpart of the semiclassical picture of the E1 giant resonance.[104,105]

A. TRM prediction of the scissors mode

The Hamiltonian describing two axially symmetric rotors interacting via a potential $V(\vartheta)$ dependent on the angle 2ϑ between the symmetry axes has the form

$$H_{\mathrm{TR}}=\frac{1}{2\mathfrak{J}_p}\,\mathbf{J}_p^2+\frac{1}{2\mathfrak{J}_n}\,\mathbf{J}_n^2+V(\vartheta), \tag{2.1}$$

where $\mathfrak{J}_p$ and $\mathfrak{J}_n$ are the proton and neutron moments of inertia, and $\mathbf{J}_p$ and $\mathbf{J}_n$ are their angular momenta. Expressed in terms of the total and relative angular momenta

$$\mathbf{J}=\mathbf{J}_p+\mathbf{J}_n, \quad \mathbf{S}=\mathbf{J}_p-\mathbf{J}_n, \tag{2.2}$$

the Hamiltonian decouples into a rotational and an intrinsic part, if a Coriolis-like term is neglected. For small values of ϑ, the intrinsic part assumes the form of a two-dimensional harmonic-oscillator (HO) Hamiltonian

$$H=H_{\mathrm{int}}=\frac{1}{2\mathfrak{J}_{\mathrm{sc}}}\,(S_1^2+S_2^2)+\frac{1}{2}\,C_\vartheta(\vartheta_1^2+\vartheta_2^2), \tag{2.3}$$

where ϑ_k $(k=1,2)$ play the role of x and y variables, and

$$S_k=J_k^{(p)}-J_k^{(n)}=i\,\frac{d}{d\vartheta_k} \tag{2.4}$$

are their conjugate momenta. The TRM physical constants are

$$\mathfrak{J}_{\mathrm{sc}}=\frac{4\mathfrak{J}_p\mathfrak{J}_n}{\mathfrak{J}_p+\mathfrak{J}_n}, \quad C_\vartheta=\mathfrak{J}_{\mathrm{sc}}\omega^2=\frac{4C_\vartheta^{(p)}C_\vartheta^{(n)}}{C_\vartheta^{(p)}+C_\vartheta^{(n)}}, \tag{2.5}$$

where we have put $C_\vartheta^{(\tau)}=\omega^2\mathfrak{J}_\tau$, with $\tau=p$ for protons and $\tau=n$ for neutrons.

The energy eigenvalues are

$$\omega_{nK}=\omega(2n+K+1). \tag{2.6}$$

The scissors mode corresponds to the first excited level. Its quantum numbers $n=0$ and $K=1$ define a positive-parity band of intrinsic excitation energy ω. In order to illustrate the mechanism of excitation we decompose the TRM M1 operator as follows:

$$\mathscr{M}(M1,\mu)=\sqrt{\frac{3}{4\pi}}\,(g_pJ_\mu^{(p)}+g_nJ_\mu^{(n)})\mu_N$$
$$=\mathscr{M}_J(M1,\mu)+\mathscr{M}_{\rm sc}(M1,\mu). \tag{2.7}$$

The first part is the rotational component

$$\mathscr{M}_J(M1,\mu)=\sqrt{\frac{3}{4\pi}}\,J_\mu g_R\mu_N, \tag{2.8}$$

where $g_R=(g_p+g_n)/2$ is the rotational gyromagnetic factor. The second is the scissors M1 component

$$\mathscr{M}_{\rm sc}(M1,\mu)=\sqrt{\frac{3}{16\pi}}\,S_\mu g_r\mu_N, \tag{2.9}$$

where $g_r=g_p-g_n$. This term is responsible for the excitation of the mode. In order to compute the transition strength one may exploit the harmonic relations holding for the TRM Hamiltonian:

$$\frac{1}{\mathfrak{J}_{\rm sc}}\langle S^2\rangle=\frac{1}{\mathfrak{J}_{\rm sc}}\sum_{\mu=\pm1}|\langle\mu|S_\mu|0\rangle|^2=\omega,$$

$$C=\omega\sum_{\mu=\pm1}|\langle\mu|S_\mu|0\rangle|^2. \tag{2.10}$$

In view of the structure of the scissors M1 operator (2.9), the above equations yield, for the M1 strength, the expression

$$B(M1)\uparrow=\frac{3}{16\pi}\sum_{\mu=\pm1}|\langle\mu|S_\mu|0\rangle|^2g_r^2\mu_N^2$$
$$=\frac{3}{16\pi}\,\mathfrak{J}_{\rm sc}\omega g_r^2\mu_N^2. \tag{2.11}$$

The mode can be further characterized by the M1 form factor. The general expression for the magnetic orbital operator for electron scattering is

$$T_\mu^{(\lambda)}(q)=-\frac{i}{\sqrt{\lambda(\lambda+1)}}\int d\mathbf{r}\mathbf{j}_p(\mathbf{r})\cdot\mathbf{r}\times\boldsymbol{\nabla}(j_\lambda(qr)Y_{\lambda\mu})$$
$$=-\frac{i}{\sqrt{\lambda(\lambda+1)}}\int d\mathbf{r}\rho_p(\mathbf{r})\mathbf{v}_p(\mathbf{r})\cdot(\mathbf{r}\times\boldsymbol{\nabla})$$
$$\times(j_\lambda(qr)Y_{\lambda\mu})$$
$$=-\frac{1}{m}\frac{i}{\sqrt{\lambda(\lambda+1)}}\int d\mathbf{r}\rho_p(\mathbf{r})\mathbf{l}_p\cdot\boldsymbol{\nabla}(j_\lambda(qr)Y_{\lambda\mu}), \tag{2.12}$$

where m and $\mathbf{l}_p$ are the proton mass and angular momentum, respectively.

The transition operator can be conveniently rewritten by using the classical relations

$$\mathbf{l}=m\mathbf{r}(\mathbf{r}\cdot\boldsymbol{\Omega})-mr^2\boldsymbol{\Omega},$$
$$\boldsymbol{\Omega}_p=\frac{1}{\mathfrak{J}_p}\,\mathbf{I}_p. \tag{2.13}$$

After some straightforward algebra we obtain ($\mu=\pm1$)

$$T_\mu^{(\lambda)}(q)=\frac{i}{\sqrt{2\lambda(\lambda+1)}}\,S_\mu\,\frac{1}{\mathfrak{J}_p}\int d\mathbf{r}\rho_p(\mathbf{r})\,\frac{j_\lambda(qr)}{r^\lambda}\,(r^2\partial_1$$
$$-x_1\mathbf{r}\cdot\boldsymbol{\nabla})(r^\lambda Y_{\lambda\mu}). \tag{2.14}$$

For $\lambda=1$ the only nonvanishing matrix element is

$$\langle I=K=1,\ n=0\|T^{(\lambda)}(q)\|I=K=n=0\rangle$$
$$=-\sqrt{\frac{\pi}{3}}\sqrt{\frac{\omega}{\mathfrak{J}}}\int_0^\infty drr^3\rho(r)j_1(qr), \tag{2.15}$$

where $\rho(r)$ is a spherical density, normalized to the total number of nucleons.

For $\lambda>1$ the integral in Eq. (2.14) vanishes unless the density deformation is taken into account. For this purpose[106] let us consider a proton (neutron) density of the form suitable for an axially deformed shape:

$$\varrho_\tau(\mathbf{r})=\varrho_\tau[r-R(1+\alpha_{20}^{(\tau)}Y_{20}(\hat{r}))], \tag{2.16}$$

where

$$\alpha_{20}^{(\tau)}=\beta_\tau=\sqrt{\frac{16\pi}{45}}\,\delta_\tau. \tag{2.17}$$

For $\lambda=3$ the only nonvanishing matrix element is[106]

$$\langle I=3,\ K=1,\ n=0\|T^{(\lambda=3)}(q)\|I=K=n=0\rangle$$
$$=\frac{4}{15}\sqrt{\frac{2\pi}{7}}\,\delta\sqrt{\frac{\omega}{\mathfrak{J}}}q\int drr^4\rho(r)j_2(qr). \tag{2.18}$$

The M3 transition strength can be obtained by going to the photon point and turns out to be related to the M1 transition probability by

$$B(M3)\uparrow=1.14\delta^2R^4B(M1)\uparrow. \tag{2.19}$$

B. Experimental evidence and characterization of the mode

A level with the properties of the $J^\pi=1^+$, $K^\pi=1^+$ state predicted by the TRM was discovered in a high-resolution (e,e') experiment on ^{156}Gd by the group of Richter.[1] The M1 excitation was detected by performing (e,e') scattering at backward angles ($\theta=165°$), where transverse magnetic transitions are dominant. The experimental form factor of this state is in close agreement with the TRM up to moderately high values of the momentum transfer q. The discrepancy at high q values can be attributed to spin contributions, absent in the TRM.[107,108]

Soon after, this strongly excited state was confirmed in (γ,γ') experiments.[109] In these reactions the decay of the $J^\pi=1^+$ state to the $J^\pi=2_1^+$ level of the ground-state band was also observed. This made it possible to determine the K value of the state under investigation, using the Alaga rule.[110] In fact, in the rotational limit we have

$$R=\frac{B(M1,1^+\to 2_1^+)}{B(M1,1^+\to 0^+)}=\frac{|\langle 1K\lambda-K|2\ 0\rangle|^2}{|\langle 1K\lambda-K|0\ 0\rangle|^2}. \tag{2.20}$$

This ratio is $R=0.5$ if $K=1$, and $R=2$ if $K=0$. Experimentally, R is about 0.5, which is consistent with the $K=1$ assignment.

Subsequent inelastic electron scattering and NRF experiments have ascertained the existence of the mode in three regions of the nuclear table, i.e., the deformed rare-earth nuclei,[111–119] the fp-shell nuclei,[120-122] and the actinides.[123,124] However, most of the experimental studies were performed on rare-earth nuclei.

We have already pointed out that the electron-scattering form factors are in good agreement with the predictions based on the assumption that the excitation mode is of orbital nature. Further support for this property of the mode has been gained by comparing the (e,e') with the (p,p') scattering.[120,125,126] In (p,p') reactions, in fact, the intermediate-energy proton scattering at small angles excites magnetic dipole states only through the spin part of the nucleon–nucleon interaction. The fact that the M1 states observed in electron scattering are not appreciably excited in the (p,p') reaction provides strong evidence in favor of the orbital nature of the mode.

A combined analysis of (e,e') and (γ,γ') experiments[127] has shown that the mode is fragmented into several peaks closely packed around a prominent one with a total strength $B(M1)\uparrow\simeq 3\mu_N^2$. Attempts to clarify the nature of the single peaks have been made through (t,α) reactions.[128,129]

Joint (e,e') and (γ,γ') experiments carried out on a chain of even Sm isotopes have shown that the integrated M1 strength grows quadratically with the deformation parameter[11] and is proportional to the strength of the E2 transition to the lowest 2^+ state.[12] The same deformation law was confirmed in Nd isotopes[13] and has now been ascertained to hold for all nuclei of the rare-earth region.[14,15] The experiments on some actinides indicate that there is evidence for a δ^2 law also in this region.[10,130] This law is perhaps the most spectacular manifestation of the scissors nature of the M1 transitions.

This systematic study was possible by virtue of the great progress made in gamma spectroscopy. Indeed, the measurement of the linear polarization of the scattered photons in nuclear-resonance fluorescence (NRF) experiments has enabled parity assignment[17] and, thereby, the unambiguous identification of the M1 transitions.[17–20] The same experiments have established the existence of E1 transitions intermixed with M1 excitations.

The experimental setups have now increased the detection sensitivity to a point at which very weak transitions can be identified. A first success was the discovery of scissors-like excitations in γ-soft nuclei.[131,132]

The present status of the experimental results can be found in several review articles.[6–10] The salient features of the mode which can be extracted from them are:

•The M1 strength is fragmented and distributed around an energy centroid, which assumes the value $\omega\simeq 3$ MeV in rare-earth nuclei.

•The summed strength in the most deformed rare-earth nuclei is $\Sigma B(\mathrm{M1})\uparrow\simeq 3\mu_N^2$.

•The transition is mainly promoted by the convection current. The orbital-to-spin ratio is typically $B_l(\mathrm{M1})/B_\sigma(\mathrm{M1})\simeq 10$.

•The integrated M1 strength depends quadratically on the deformation parameter and is strictly correlated with the strength of the E2 transition to the lowest 2^+ state.

While qualitatively consistent with the observed properties of the mode, the TRM, in its original formulation,[2] was unable to predict either the exact position of the energy centroid or the size of the total strength. Indeed, the TRM energy was higher than the observed one by about 1 MeV, and the M1 strength was five times larger. The main reason for these strong discrepancies is to be found in the crude numerical estimates of the model parameters made in that paper. A rigid-body moment of inertia was assumed, and the restoring-force constant was computed by paralleling the procedure adopted by Goldhaber and Teller for the E1 giant resonance. We know now that both prescriptions are unrealistic. There is, however, little doubt that the mode predicted by the model corresponds to the observed M1 excitations. We have already said that the experimental form factor is reproduced by the model to a large extent. We will see now that the model is also consistent with the quadratic deformation law.

C. Consistency of the TRM with the deformation law

As pointed out already, the most meaningful signature of the observed M1 transitions is the quadratic deformation law for the total M1 strength. It is therefore of the utmost importance to investigate whether the TRM can predict such a behavior. For this purpose it is useful to express all TRM quantities in terms of the shape variables $\alpha_{2\mu}$ instead of the angle ϑ and to impose on the proton (neutron) density (2.16) the normalization condition

$$\langle Q_{\lambda\mu}^{(\tau)}\rangle=\int \varrho_\tau(\mathbf{r})r^\lambda Y_{\lambda\mu}(\mathbf{r})d\mathbf{r}=\alpha_{\lambda\mu}\varrho_0^{(\tau)}R^{\lambda+3}, \tag{2.21}$$

where $\varrho_0^{(p)}$ and $\varrho_0^{(n)}$ are normalized to the number of protons and neutrons, respectively. Under a rotation by ϑ_τ ($\vartheta_p=\vartheta$, $\vartheta_n=-\vartheta$) around the x axis, the proton ($\tau=p$) and neutron ($\tau=n$) densities undergo the following change:

$$\varrho_\tau(R_{\vartheta_\tau}^{-1}\mathbf{r})=\varrho_\tau\left[r-R\left(1+\sum_{\mu=\pm 1}\alpha_{2\mu}^{(\tau)}Y_{2\mu}^*(\hat{r})\right)\right], \tag{2.22}$$

where

$$\alpha_{2\mu}^{(\tau)}=D_{0\mu}^{(2)}(\vartheta_\tau)\alpha_{20}^{(\tau)}\simeq -i\sqrt{\frac{3}{2}}\,\alpha_{20}^{(\tau)}\vartheta_\tau=-i\sqrt{\frac{3}{2}}\,\beta_\tau\vartheta_\tau \tag{2.23}$$

to leading order in ϑ_τ. This key relation enables us to express the TRM Hamiltonian (2.3) in terms of shape variables, namely,

$$H=\frac{1}{2\mathfrak{J}_{\mathrm{sc}}}S^2+\frac{1}{2}C_\vartheta\vartheta^2=\frac{1}{2B_{\mathrm{sc}}}\sum_{\mu=\pm 1}|\pi_{2\mu}|^2$$

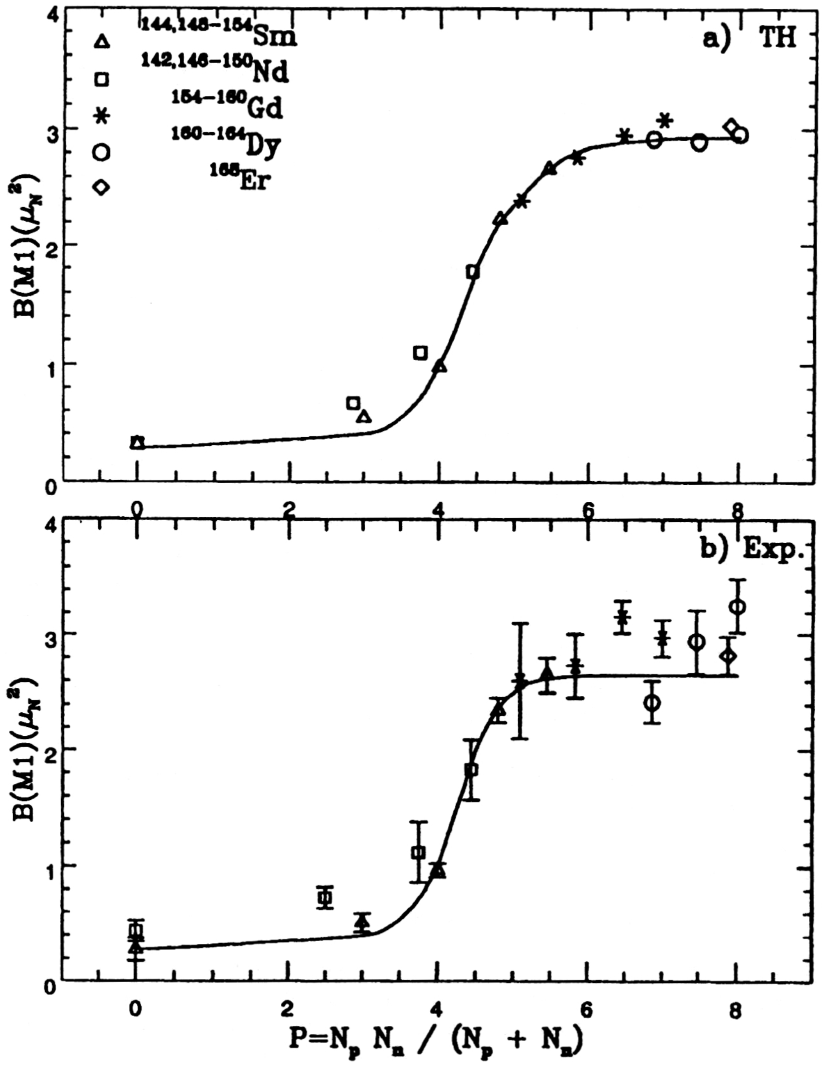

FIG. 1. Saturation plot of the scissors M1 strength computed using the TRM formula (2.28). The quantity P is the Casten number defined in the text [Eq. (3.32)].

$$+\frac{1}{2}C\sum_{\mu=\pm1}|\alpha_{2\mu}|^2, \tag{2.24}$$

where $\pi_{2\mu}$ are conjugate to $\alpha_{2\mu}$, and

$$B_{\rm sc}=\frac{4B_pB_n}{B_p+B_n},\quad C=\frac{4C_pC_n}{C_p+C_n} \tag{2.25}$$

are the new model parameters. The old and new constants are related by

$$\mathfrak{J}_\tau=3\beta_\tau^2B_\tau,\quad C_\vartheta^{(\tau)}=3\beta_\tau^2C_\tau. \tag{2.26}$$

It follows by inspection that, while the energy is independent of the deformation, the scissors M1 strength grows quadratically with it. Indeed, upon insertion of the above expressions into the TRM harmonic relations (2.10), the scissors strength (2.11) becomes

$$B_{\rm sc}(M1)\uparrow=\frac{9}{16\pi}B\omega\beta^2g_r^2\mu_N^2. \tag{2.27}$$

The δ^2 behavior of the scissors M1 strength has been studied quantitatively in Ref. 90 by making an empirical estimate of the mass parameter. The following expression was obtained:

$$B_{\rm sc}(M1)\uparrow\simeq0.004\omega A^{5/3}\delta^2g_r^2\mu_N^2. \tag{2.28}$$

Numerical calculations carried out by putting $g_n=0$ and $g_r=g_p=2g_R=(2Z)/A$ yield results in good agreement with experiments.[11–13] In particular, the theoretical and experimental summed M1 strengths have similar saturation properties (Fig. 1). A systematic analysis carried out recently[14,15] has shown that the M1 strengths computed by such an empirical formula are in overall agreement with experiments for all nuclei of the whole rare-earth region. The formula has been shown to account also for the deformation dependence of the M1 strength in actinide isotopes[10,130] and in γ-soft nuclei.[131,132]

D. Thoretical computation of the TRM constants: a low- and a high-energy mode

1. Classical method

Within the semiclassical domain one may attach to each of the two rotors the velocity fields

$$\mathbf{v}_p=-\nabla\chi_p,\quad \mathbf{v}_n=-\nabla\chi_n, \tag{2.29}$$

where

$$\chi_\tau = \delta(x_{2_\tau} x_{3_\tau} \Omega_{1_\tau} + x_{1_\tau} x_{3_\tau} \Omega_{2_\tau}), \tag{2.30}$$

in which Ω_{i_τ} ($i_\tau = x_\tau, y_\tau$) are the proton and neutron angular velocities. One obtains a two-rotor Hamiltonian of the form given by Eq. (2.1) and therefore an intrinsic one given by Eq. (2.3) with an irrotational moment of inertia

$$\mathfrak{J}_{sc} = \mathfrak{J}_{irr} = \delta^2 \mathfrak{J}_{rig}, \quad \mathfrak{J}_{rig} \simeq \frac{2}{5} mAR^2. \tag{2.31}$$

The restoring-force constant can be deduced from the symmetry-energy mass formula

$$\Delta V = \frac{1}{2} b_s \int \frac{(\delta \varrho)^2}{\varrho_0} d\mathbf{r} = \frac{1}{2} b_s \int \frac{(\delta \varrho_p - \delta \varrho_n)^2}{\varrho_0} d\mathbf{r}, \tag{2.32}$$

where $b_s \simeq 50$ MeV and ϱ_0 is the nuclear density, normalized to the mass number. The density variation is computed by making use of Eq. (2.22), with the result

$$\delta \varrho_\tau = \varrho_\tau(\vartheta_\tau) - \varrho_\tau(0) = k_\tau \varrho_0^{(\tau)} \sum_{\mu = \pm 1} \alpha_{2\mu}^{(\tau)} r^2 Y_{2\mu}^*, \tag{2.33}$$

where the constant k_τ is fixed by the normalization condition (2.21), and $\alpha_{2\mu}^{(\tau)}$ is given by Eq. (2.23). The calculation of the integral in Eq. (2.32) then yields

$$\Delta V = \frac{1}{2} C \vartheta^2, \tag{2.34}$$

where

$$C \simeq \frac{28}{5} b_s A \delta^2. \tag{2.35}$$

Using the above equations, one obtains, for the energy of the mode and the corresponding strength [Eq. (2.11)],

$$\omega_+ \simeq 139.4 A^{-1/3} \text{ MeV},$$

$$B_+(M1)\uparrow \simeq 0.12 \delta^2 A^{4/3} g_r^2 \mu_N^2. \tag{2.36}$$

The strength is quadratic in the deformation parameter, but the energy is far higher than the observed one. Indeed, we obtain for ^{154}Sm the values $\omega \simeq 26$ MeV and $B(M1)\uparrow \simeq 4.7 \mu_N^2$, having put $g_n = 0$ and $g_p = 2g_R = 2Z/A$. Although the M1 strength is reasonably close to the experimental value, the energy lies in the region of the giant isovector quadrupole resonance. What we have found is actually a new scissors mode. It is indeed the $K^\pi = 1^+$ component of the isovector quadrupole resonance mode. In order to obtain a low-energy mode one has to make different assumptions about the nature of the rotors. A natural prescription for all possible alternatives can be found once the model is formulated in a microscopic context.

2. Microscopic approach: equivalence with the schematic RPA

Let us assume that the nucleons move in a deformed mean field described by an anisotropic HO potential with frequencies ω_1 and ω_3 such that $\omega_1^2 \omega_3 = \omega_0^3$ and $\omega_0 \simeq 41 A^{-1/3}$ MeV.

Mapping the procedure of the Bohr and Mottelson unified theory[133] to the present case, one can make use of the harmonic relations (2.10) in the specific form

$$\frac{1}{\mathfrak{J}_{sc}} \langle S^2 \rangle = \frac{1}{\mathfrak{J}_{sc}} \sum_{ph \in 2\omega_0} \sum_{\mu \pm 1} |\langle ph | S_\mu | \rangle|^2 = \omega_1 + \omega_3 \simeq 2\omega_0, \tag{2.37}$$

where $|\rangle$ is the particle–hole ($p-h$) vacuum. The sum is restricted to the $\Delta N = 2$ $p-h$ excitations. This condition yields the irrotational mass parameter

$$\mathfrak{J}_{sc} = \mathfrak{J}_{irr} = \delta^2 \mathfrak{J}_{rig}, \quad \mathfrak{J}_{rig} = \frac{1}{\delta \omega_0} \sum_{ph \in \delta\omega_0} |(S_+)_{ph}|^2$$

$$\simeq \frac{2}{5} mAR^2, \tag{2.38}$$

and the restoring-force constant

$$C_0^{(+)} \simeq \mathfrak{J}_{irr} (2\omega_0)^2 \simeq \frac{28}{5} b_0 A \delta^2, \tag{2.39}$$

where $b_0 \simeq 17.5$ MeV. When the $p-h$ interaction is switched on, the restoring-force constant acquires the additional contribution

$$C_1^{(+)} \simeq \frac{28}{5} b_1 A \delta^2, \tag{2.40}$$

where the constant b_1 follows from its relation to the energy symmetry potential $V_1 = 4b_1 \simeq 130$ MeV. The full restoring-force constant $C_+ = C_0^{(+)} + C_1^{(+)}$ turns out to be exactly equal to the classical expression (2.35) with the same symmetry parameter $b_s = b_0 + b_1 \simeq 50$ MeV. It follows that the resulting energy and strength are given exactly by the semiclassical equations (2.36).

We use now Eq. (2.10) with the following requirement:

$$\frac{1}{\mathfrak{J}_{sc}} \langle S^2 \rangle = \frac{1}{\mathfrak{J}_{sc}} \sum_{ph \in \delta\omega_0} \sum_{\mu = \pm 1} |\langle ph | S_\mu | \rangle|^2 \simeq \delta \omega_0, \tag{2.41}$$

where the sum is restricted to the $\Delta N = 0$ $p-h$ space. This yields a rigid-body moment of inertia $\mathfrak{J}_{sc} = \mathfrak{J}_{rig}$. The unperturbed restoring-force constant is now

$$C_0^{(-)} \simeq (\delta\omega_0)^2 \mathfrak{J}_{rig} = \frac{28}{5} b_0^{(-)} A \delta^2 \tag{2.42}$$

with $b_0^{(-)} \simeq b_0/4$. The potential component can be fixed[133] from the ratio of the nuclear isovector and isoscalar average potential strengths V_1 and V_0, $a_- = C_1^{(-)}/C_0^{(-)} = b_1^{(-)}/b_0^{(-)} = -V_1/(4V_0) \simeq 0.6$. The final result is

$$\omega_- = \sqrt{\frac{C_-}{\mathfrak{J}_{rig}}} = \delta\omega_0 \sqrt{1 + a_-} \simeq 53 \delta A^{-1/3} \text{ MeV}, \tag{2.43}$$

$$B_-(M1)\uparrow \simeq \frac{3}{4\pi} \mathfrak{J}_{rig} \omega_- \simeq 0.045 \delta A^{4/3} g_r^2 \mu_N^2.$$

The method just developed is nearly equivalent to the entirely classical one adopted in the TRM in its original formulation.[2] Both rely on the assumption that protons and neutrons form two rigid rotors. The present method, however, improves the computation of the restoring-force constant, with the result that the M1 strength is reduced by about a factor of two. Such a reduction, however, is not enough. In order to induce a further quenching, one needs to remove the rigid-body assumption.

For this purpose one may impose for the low-energy mode the alternative condition

$$\frac{1}{\mathfrak{J}_{sc}}\langle S^2\rangle = E(\epsilon_{sp}) + E(\epsilon_{sp}+\delta\omega_0), \tag{2.44}$$

where $E(\epsilon_{sp}) = \sqrt{(\epsilon_{sp}-\lambda)^2+\Delta^2}$ is the quasiparticle energy. Here, ϵ_{sp} is the single-particle (s.p.) energy, referred to the chemical potential λ, and Δ is the pairing gap. It is natural to use for λ the value $\lambda = (\delta\omega_0)/2$. With this choice the harmonic condition (2.10) becomes

$$\frac{1}{\mathfrak{J}_{sc}}\langle S^2\rangle = 2E = \sqrt{(\delta\omega_0)^2+(2\Delta)^2}. \tag{2.45}$$

Using closure, we obtain for the mass parameter

$$\mathfrak{J}_{sc} \simeq \mathfrak{J}_{sf} \simeq \frac{\delta\omega_0}{(2E)}\Big(u(\epsilon_{sp})v(\epsilon_{sp}+\delta\omega_0) - (v(\epsilon_{sp})u(\epsilon_{sp} + \delta\omega_0))^2\mathfrak{J}_{rig} \simeq \left(\frac{\delta\omega_0}{2E}\right)^3 \mathfrak{J}_{rig}, \tag{2.46}$$

having made use of the standard expressions of the BCS amplitudes u and v with $\lambda = (\delta\omega_0)/2$. The resulting energy and strength are

$$\omega_- = \sqrt{\frac{C_-}{\mathfrak{J}_{sf}}} \simeq (2E)\sqrt{1+a_-},$$

$$B_-(M1)\uparrow \simeq \frac{3}{16\pi}\,\omega_-\mathfrak{J}_{rig}\left(\frac{\delta\omega_0}{2E}\right)^3 g_r^2\mu_N^2, \tag{2.47}$$

or, more explicitly,

$$\omega_- \simeq 1.26(2\Delta)\sqrt{1+x^2},$$

$$B_-(M1)\uparrow \simeq 0.001(2\Delta)A^{5/3}\frac{x^3}{1+x^2}g_r^2\mu_N^2, \tag{2.48}$$

where $x = \delta\omega_0/(2\Delta)$. According to these equations, the strength goes like δ^3 for small deformations ($x \ll 1$) and becomes linear for very large deformations ($x \gg 1$). In the range of observed deformations the strength is approximately quadratic in δ.

Had we averaged the two quasiparticle energies and the moment of inertia with respect to λ,[133] we would have obtained exactly the strength derived by Hamamoto and Magnusson in the schematic RPA.[69] This is not an accident. The approach presented here amounts exactly to a schematic RPA treatment. To show this equivalence we observe that, when expressed in terms of shape variables, the intrinsic TRM Hamiltonian (2.24) coincides with the harmonic Hamiltonian adopted within the unified theory.[133] Let us indeed switch from the normalization (2.21) to the new one

$$\langle Q_{\lambda\mu}\rangle = \int \varrho(\mathbf{r})r^\lambda Y_{\lambda\mu}(\mathbf{r})d\mathbf{r} = \alpha_{\lambda\mu}. \tag{2.49}$$

This induces in turn a renormalization of the mass and restoring-force parameters, which assume the new form

$$\mathfrak{J}_{sc} \Rightarrow B_\alpha = \frac{\mathfrak{J}_{sc}}{3\beta^2\left(\frac{3}{4\pi}AR^2\right)^2} = \frac{2\pi}{3}\frac{m}{AR^2},$$

$$C_\vartheta \Rightarrow C_\alpha = \frac{C}{3\beta^2\left(\frac{3}{4\pi}AR^2\right)^2} = C_\alpha^{(0)} + C_\alpha^{(1)}, \tag{2.50}$$

where

$$C_\alpha^{(0)} \simeq \frac{8\pi}{3}\frac{m\omega_0^2}{AR^2}, \quad C_\alpha^{(1)} \simeq \frac{7}{3}\frac{\pi V_1}{AR^4}. \tag{2.51}$$

These quantities are just the mass parameters and coupling strengths derived within the unified-theory approach.[133]

The link with the schematic RPA is now obtained simply through the standard mapping condition[133]

$$\sum_\mu |\alpha_{2\mu}|^2 = \sum_\mu \sum_{ph} |(Q_{2\mu}(1))_{ph}|^2,$$

$$Q_{2\mu}(1) = Q_{2\mu}^{(p)} - Q_{2\mu}^{(n)}. \tag{2.52}$$

Needless to say, an explicit RPA calculation yields exactly the results obtained here.[34–36] Although the deformation dependence is roughly reproduced, the magnitude of the strength produced by these calculations is about a factor two larger than the experimental summed strength. A quenching mechanism is needed. This is hopefully found if the model can be formulated in a fully microscopic context which accounts also for the spin degrees of freedom.

3. Scissors modes in superdeformed nuclei

We have seen that, in its reformulated version, the TRM predicts a low- and a high-energy mode. In the first mode, protons and neutrons behave approximately as superfluid systems; in the second, as irrotational fluids. Being switched by deformation, the two modes should exist also in superdeformed nuclei. Their existence was indeed predicted in the RPA[72] and within the classical TRM.[134] This latter model can be easily adapted to these nuclei. Indeed, let us assume that K is a good quantum number, so that the transition goes from K to $K+1$. The M1 operator couples the state $|IMK\rangle$ to the states $|I'M'K+1\rangle$ with $I' = I-1, I, I+1$. Using the standard expression for the transition matrix elements[133] with the TRM intrinsic wave function[2] and assuming $I \gg K$, we obtain for the summed strength

$$\sum_{I'} B(M1,\, IK \to I'K+1) \simeq \frac{3}{16\pi}\mathfrak{J}_{sc}\omega\frac{1}{K+1}g_r^2\mu_N^2. \tag{2.53}$$

According to this expression, the strength decreases with increasing K. If we assume that the superdeformed state has $K=0$, we gain the standard scissors expression (2.11). We may use Eqs. (2.36), obtaining for the high-energy mode of the superdeformed ^{152}Dy ($\delta \simeq 0.62$) the values

$$\omega_+ \simeq 26\ \text{MeV}, \quad B_+(M1)\uparrow \simeq 26.1\mu_N^2, \tag{2.54}$$

where we have put $g_n = 0$ and $g_p = 2g_R = 2Z/A$.

For the low-energy mode we may assume rigid rotors and use Eqs. (2.48) with $g_n=0$ and $g_p=1$, obtaining for the same superdeformed nucleus the values

$$\omega_- \simeq 6.1\ \text{MeV}, \quad B_-(M1)\uparrow \simeq 22.6\mu_N^2. \tag{2.55}$$

These numbers are in agreement with the RPA results of Ref. 72. They have been obtained under the assumption that, in going from deformed to superdeformed nuclei, protons and neutrons in their relative motion remain irrotational at high energy but undergo a transition from a superfluid to a rigid-body phase at low energy. Such an assumption is fully consistent with the conclusions drawn in Ref. 72.

We would like to stress that, according to our equations based on the use of the TRM scissors wave function, these strong transitions occur only if the intrinsic superdeformed state has $K=0$. If such a state has a nonvanishing but small K, or contains a K admixture, the corresponding strength should still be sizable.

4. M1 mode in triaxial nuclei

The model can be easily extended to triaxial nuclei.[135,136] For this purpose one can easily deduce the quadrupole fields entering into the M1 channel from the density variation induced by the rotation of protons against neutrons around each of the three principal axes. They are

$$\begin{aligned} Q_1 &= -\frac{i}{\sqrt{2}} r^2 (Y_{21}+Y_{2-1})\tau_3, \\ Q_2 &= -\frac{1}{\sqrt{2}} r^2 (Y_{21}-Y_{2-1})\tau_3, \\ Q_3 &= \frac{-i}{\sqrt{2}} r^2 (Y_{22}-Y_{2-2})\tau_3. \end{aligned} \tag{2.56}$$

The corresponding excitation energies are

$$\begin{aligned} \epsilon_1^{(\pm)} &= |\omega_2 \pm \omega_3| = \omega_0 |e^{-\alpha\cos(\gamma-4\pi/3)} \pm e^{-\alpha\cos\gamma}|, \\ \epsilon_2^{(\pm)} &= |\omega_1 \pm \omega_3| = \omega_0 |e^{-\alpha\cos(\gamma-2\pi/3)} \pm e^{-\alpha\cos\gamma}|, \\ \epsilon_3^{(\pm)} &= |\omega_1 \pm \omega_2| = \omega_0 |e^{-\alpha\cos(\gamma-2\pi/3)} \\ &\quad \pm e^{-\alpha\cos\gamma(\gamma-4\pi/3)}|. \end{aligned} \tag{2.57}$$

The lowest eigenvalues for each mode are

$$\begin{aligned} \omega_i &= \omega \cos\gamma \left(1 - \frac{(-1)^i}{\sqrt{3}} \tan\gamma\right) \quad (i=1,2), \\ \omega_3 &= \frac{2}{\sqrt{3}}\omega \sin\gamma. \end{aligned} \tag{2.58}$$

We have neglected pairing for simplicity.

The E2 and M1 strengths are

$$\begin{aligned} B_i(E2) &= \frac{1}{2}\cos\gamma \left(1 - \frac{(-1)^i}{\sqrt{3}} \tan\gamma\right) B(E2) \quad (i=1,2), \\ B_3(E2) &= \frac{2}{\sqrt{3}} \sin\gamma B(E2), \end{aligned} \tag{2.59}$$

$$\begin{aligned} B_i(M1) &= \frac{1}{2}\cos\gamma \left(1 - \frac{(-1)^i}{\sqrt{3}} \tan\gamma\right) B(M1), \\ B_3(M1) &= \frac{2}{\sqrt{3}} \sin\gamma B(M1). \end{aligned} \tag{2.60}$$

For both kinds of transitions the ratio B_2/B_1 is

$$\frac{B_2}{B_1} = \frac{1 - \frac{1}{\sqrt{3}}\tan\gamma}{1 + \frac{1}{\sqrt{3}}\tan\gamma}. \tag{2.61}$$

A third mode, absent in axial nuclei, emerges. Its frequency and strengths contain γ as a leading term, in accord with the fact that such a mode disappears in the axial limit. For very small values of γ the frequency is very low and the strength is negligible.

According to the model predictions, a splitting of the M1 strength should signal a triaxial shape. Unfortunately, such a splitting is likely to be hidden by the fragmentation induced by the nuclear shell structure. Such a test may therefore work only in some medium-light nuclei where the fragmentation induced by the shell structure can be modest.

E. Microscopic formulation of the TRM

It is not obvious that the scissors picture should be preserved within a microscopic context. The spin degree of freedom can in fact interfere so as to destroy such a picture. This is to be expected to some extent, since the spin–orbit coupling induces a large fragmentation in the s.p. spectrum. In order to check whether the scissors picture still holds, it is useful to analyze the excitation mechanism. The full shell-model M1 operator is

$$\mathcal{M}(M1,\mu) = \sqrt{3/(4\pi)} \sum_{i=1}^{A} (g_l(i) l_\mu(i) + g_s(i) s_\mu(i))\mu_N. \tag{2.62}$$

The scissors picture remains valid only if the spin contribution is negligible or can be absorbed into the generator S, so that the M1 operator can be written in the TRM form

$$\mathcal{M}(M1,\mu=1) = \left(\frac{3}{16\pi}\right)^{1/2} S_{+1}(g_p - g_n)\mu_N. \tag{2.63}$$

In such a case general definitions of the TRM constants which are valid in any microscopic context can be given easily. For this purpose it is useful to write the defining TRM equation (2.10) in the form[34]

$$\begin{aligned} \mathfrak{I}_{\text{sc}} &= \sum_{\mu=\pm1} \left\langle 0 \left| S_\mu^\dagger \frac{1}{H-E_0} S_\mu \right| 0 \right\rangle, \\ C &= \frac{1}{2} \sum_{\mu=\pm1} \langle 0 | [S_\mu^\dagger, [H, S_\mu]] | 0 \rangle. \end{aligned} \tag{2.64}$$

Using closure, one obtains the quite general expressions

$$\mathfrak{J}_{sc}=\sum_{n\mu}\frac{1}{\omega_n}|\langle n\mu|S_\mu|0\rangle|^2,$$
$$C=\sum_{n\mu}\omega_n|\langle n\mu|S_\mu|0\rangle|^2. \tag{2.65}$$

We can now immediately derive the scissors energy-weighted M1 sum rule

$$\sum_n \omega_n B_n(M1)\uparrow=\frac{3}{16\pi}\sum_{n,\mu}\omega_n|\langle n\mu|S_\mu|0\rangle|^2 g_r^2\mu_N^2$$
$$=\frac{3}{32\pi}\sum_{\mu=\pm1}\langle 0|[S_\mu^+,[H,S_\mu]]|0\rangle g_r^2\mu_N^2$$
$$\simeq\frac{3}{16\pi}\mathfrak{J}_{sc}\omega^2 g_r^2\mu_N^2. \tag{2.66}$$

This sum rule holds in the macroscopic as well as in the microscopic domain. Under the experimentally supported assumption of small fragmentation of the mode, we obtain for the summed strength the expression defining the TRM M1 strength [Eq. (2.9)]. It follows that the TRM formula, with $\mathfrak{J}_{sc}$ and C given by Eq. (2.65), represents a general definition of the scissors M1 summed strength. Microscopic studies of these formulas have been carried out in Ref. 137.

3. BOSON-MODEL DESCRIPTIONS

The TRM was formulated specifically for identifying a collective mode of scissors nature and predicting its signature. Hence the simplifying assumption that neutrons and protons form two fluids of ellipsoidal shape. On the other hand, the mode can be fully understood only if studied in more realistic approaches which include additional degrees of freedom. An obvious extension consists in allowing for surface vibrations of proton and neutron deformed fluids. This is accomplished within a semiclassical context by describing these vibrations in terms of the shape variables α_p and α_n. These are indeed the classical variables adopted in the phenomenological models described in this section.

A. Extended Bohr–Mottelson models

The TRM Hamiltonian, when written in terms of the Bohr–Mottelson collective variables (2.24), assumes the form adopted by Faessler and co-workers[30] to study the mode. In their approach the TRM Hamiltonian was derived from the proton–neutron Hamiltonian introduced within the extended Bohr–Mottelson model developed by Faessler himself to describe the E2 giant resonances.[138] The novelty of this model consisted in the introduction of collective variables for protons (α_p) and neutrons (α_n). Nuclear and relative motions could then be decoupled by defining the new variables

$$\alpha_\mu=\frac{1}{2}(\alpha_\mu^p+\alpha_\mu^n),\quad \xi_\mu=\alpha_\mu^p-\alpha_\mu^n. \tag{3.1}$$

The α_μ coordinates are quadrupole shape variables describing the motion of the nucleus as a whole, while the ξ_μ account for the relative motion between the proton and neutron fluids.

In their study of the scissors mode,[30] the authors started from a Hamiltonian of the form (2.24), and by using a relation similar to the one given by Eq. (2.23) they obtained a TRM Hamiltonian of the form (2.3). They improved the rigid TRM results[2] by assuming that the motion is determined by only a fraction of the nucleons. Because of this ansatz, the moment of inertia and the restoring-force constant are reduced by about a factor of three. Their M1 strength turned out to be only twice the observed one.

The same formalism was adopted by Rohozinski and Greiner[31] in a more extended framework. In fact, they formulated the problem in the laboratory frame, using a highly anharmonic Hamiltonian in the variables α_μ and ξ_μ. For small-amplitude oscillations the Hamiltonian can be decomposed into

$$H=H_{coll}(\alpha)+H_{rel}(\xi)+H_{int}(\alpha,\xi), \tag{3.2}$$

where H_{coll} describes the mass collective motion, H_{rel} is a harmonic Hamiltonian in the relative coordinates ξ_μ, and H_{int} is an interaction term which couples the two motions.

A similar decomposition holds for the total angular momentum:

$$L_{1\mu}=L_{1\mu}^n(\alpha_n)+L_{1\mu}^p(\alpha_p)=L_{1\mu}^{coll}(\alpha)+L_{1\mu}^{rel}(\xi). \tag{3.3}$$

Transforming to the intrinsic frame defined by the principal axes of the system, the variables α_μ become the Euler angles (α,β,γ) and the intrinsic shape variables a_{20} and a_{21}, while the transformed relative coordinates ξ_μ remain still five in number. In the strong-coupling limit one can put in the interaction term the equilibrium values appropriate for an axially symmetric shape, namely, $a_{20}=\beta$ and $a_{22}=0$. In this limit the transformed Hamiltonian becomes

$$H=H_{rot}+H_{\beta\gamma}+H_{centr}+H_{Coriolis}+H_{sc}. \tag{3.4}$$

Here H_{rot} and $H_{\beta\gamma}$, describing, respectively, the nuclear rotation and the β and γ vibrations around an equilibrium spheroidal shape of deformation β, form essentially the Bohr Hamiltonian,[133] while H_{centr} and $H_{Coriolis}$ are the centrifugal and Coriolis terms. The last part is the scissors Hamiltonian. This, in the strong-coupling limit, can be written

$$H_{sc}=H_{rel}(\xi)+H_{int}(\xi,\beta)=\sum_{K=0}^{2}H_K, \tag{3.5}$$

where the H_K are HO Hamiltonians in the relative coordinates and carry intrinsic angular momenta $K=0,1,2$. The coupling between the relative motion and the mass deformation mode induces a dependence of the restoring-force constant C_K and the mass parameter B_K on K and β.

The NPD model therefore predicts two other isovector modes in addition to the scissors excitation. The operator of the magnetic orbital dipole form factor is obtained from the general expression (2.14) by assuming an irrotational velocity field and a proton mass density of the form (2.16). The resulting expression is

$$T_{1\mu}^{(m)}=\frac{i}{\sqrt{2m}}\sqrt{\frac{3}{4\pi}}F(q)L_{1\mu}^p \tag{3.6}$$

with

$$F(q)=\frac{\int_0^\infty r^3 dr\left[j_1(qr)+\frac{qr}{5}j_2(qr)\right]f'(r-R_0)}{\int_0^\infty r^4 dr f'(r-R_0)}. \quad (3.7)$$

The M1 strength is obtained by going to the photon point and turns out to be of the same TRM form (2.11) with an irrotational moment of inertia. The NPD model therefore describes the mode as a rotational oscillation between two irrotational fluids.

The advantage of this model is that it describes on an equal footing the scissors as well as the β and γ vibrations and accounts for the coupling between them. The model, however, does not give clear and simple prescriptions for computing the parameters. These are in practice determined by a fit to the energy and the $B(\mathrm{M1})$ values. Another drawback is the lack of agreement between the model and experimental form factors.

The model was extended so as to make it possible to study the effect of triaxial deformation on the M1 strength.[139] It was found that, in contrast to the TRM, a small triaxiality does not lead to the appearance of 1^+ doublets.

B. Generalized coherent-state model description

The anharmonic terms of the NPD Hamiltonian are not easy to handle. An efficient approach for dealing with them is provided by the so-called coherent-state model (CSM).[140]

The idea of the CSM is to describe the low-lying collective states of spherical as well as deformed nuclei by wave functions obtained through angular-momentum projection from intrinsic coherent states, which represent a quadrupole boson condensate. The second step consists in constructing an effective interacting-boson Hamiltonian which is diagonal in the above states to a large extent. As in the NPD model, the CSM Hamiltonian is anharmonic and does not preserve the number of bosons. Because of the use of coherent states, however, such a Hamiltonian has the simplest form. This model has been used successfully to describe the collective properties of nuclei from the spherical to the transitional and deformed regions.

The M1 mode can be studied in its generalized version (GCSM),[32,33] where a distinction is made between neutron and proton bosons. The structure of the generic GCSM state is

$$\Psi_{\alpha JMK}=N_{\alpha J}P^J_{MK}\phi_{\alpha K}, \quad (3.8)$$

where $N_{\alpha J}$ is a normalization constant, and P^J_{MK} is a projection operator of standard form which projects the good angular momentum out of the intrinsic states $\phi_{\alpha K}$. These are obtained by acting with boson operators, at most quadratic in the quadrupole creation operators $b^+_{\tau\mu}$, on a HO coherent state in the deformation parameters d_p and d_n:

$$\phi_0=\exp[d_p(b^+_{p0}-b_{p0})-d_n(b^+_{n0}-b_{n0})]|\rangle. \quad (3.9)$$

States describing one β band, two γ bands, and two $K^\pi=1^+$ bands have been constructed. The one describing the scissors-mode band is

$$\Psi_{JM1}=N^J_1 P^J_{M1}(b^+_p\otimes b^+_n)_{11}|0\rangle. \quad (3.10)$$

The Hamiltonian is constructed so as to be diagonal to a good approximation in the bands of the six boson states. Its expression is

$$H=A_1(n_p+n_n)+A_2(n_{pn}+n_{np})+\sqrt{5}\,\frac{A_1+A_2}{2}(P^+_n+P^+_{np})+A_3(P^+_pP_n+P^+_nP_p-2P^+_{np}P_{np})+A_4J^2, \quad (3.11)$$

where n_p and n_n are the proton- and neutron-number operators and together with n_{pn} and n_{np} can be written in the compact form

$$n_{kk'}=\sum_\mu b^+_{k\mu}b_{k'\mu} \quad (k=p,n;\ k'=p,n), \quad (3.12)$$

P^+_p, P^+_n, and P^+_{np} are proton, neutron, and proton–neutron pairing-like boson operators

$$P^+_{kk'}=(b^+_k b^+_{k'})_0-d^2/\sqrt{5}, \quad (3.13)$$

and the quantities A_i $(i=1,4)$ are free adjustable parameters.

Equation (3.11) defines an interacting-boson Hamiltonian which does not commute with the boson-number operators n_p and n_n. Its excitation energies are obtained as

$$\omega=\langle\Psi_{1M}|H|\Psi_{1M}\rangle-\langle\Psi_0|H|\Psi_0\rangle. \quad (3.14)$$

The parameters A_i are determined from fitting some levels of the ground, β, and γ bands, while the deformation parameter, assumed equal for protons and neutrons, is fixed by an overall fit to the β band. The only free parameter is the scaling parameter entering into the canonical transformation

$$\alpha_{\tau\mu}=\frac{1}{\sqrt{2}k_\tau}(b^+_\mu+b_{\bar{\mu}}). \quad (3.15)$$

In the harmonic limit, this parameter assumes the standard form $k_\tau=\sqrt{B_\tau C_\tau}$.

The M1 operator has been derived from the general expression (2.14), using an irrotational velocity field (2.29) and a charge density of the form (2.16) as in the NPD model. The resulting expression to lowest order is

$$T(M1,\mu)=-iej_1(qR_0)(g_pJ_{p\mu}+g_nJ_{n\mu}), \quad (3.16)$$

where $J_{k,\mu}=\sqrt{10}(b^+_k b_k)_{1\mu}$. By going to the photon point, it is possible to obtain for the M1 strength a rotational and a vibrational limit[89]

$$B_{\mathrm{rot}}(M1)\uparrow=\frac{9}{4\pi}k_p^2\beta^2 g^2_{\mathrm{rel}}\mu_N^2,$$
$$B_{\mathrm{vib}}(M1)\uparrow=\frac{18}{\pi}k_p^2\beta^2 g^2_{\mathrm{rel}}\mu_N^2. \quad (3.17)$$

The result is linear in β^2 in both cases, but with two different slopes. The full GCSM expression was used to compute the M1 strength for different chains of isotopes. The experimental δ^2 behavior was nicely reproduced. If we put $k_p^2=B\omega$, valid in the harmonic approximation, we obtain for the strength in the rotational limit the TRM expression (2.27). The close link between the two approaches was discussed in Ref. 89.

The M1 form factor was computed in the plane-wave approximation.[143] Although a detailed comparison with experiments cannot be carried out, it looks promisingly close to the observed one. The octupole operator has exactly the same expression for the M1 operator with a gyromagnetic ratio $g^{(3)}_{p/n}=12/7g_{p/n}$. Once the magnetic-dipole gyromagnetic ratios are determined, the octupole ones are automatically fixed. The model predicts a scissors, an isoscalar, and an isovector M3 transition.[141] The isoscalar M3 strength is remarkably close to the one measured in ^{164}Dy and consistently interpreted as isoscalar.[142]

The GCSM has also been extended to triaxal nuclei.[143] The results are consistent with the TRM findings.

C. Algebraic description of the mode: the interacting-boson model

1. The model

The basic assumption of the interacting-boson model[144,145] is that the low-lying collective states of nuclei away from major closed shells are described in terms of a monopole boson with angular momentum and parity $J^\pi=0^+$, called an s boson, and a quadrupole boson with $J^\pi=2^+$, called a d boson. These s and d bosons are interpreted as strongly correlated pairs of valence nucleons coupled, respectively, to $J^\pi=0^+$ and $J^\pi=2^+$.

In the first formulation of the model (IBM1) no distinction is made between protons and neutrons. The Hamiltonian has the form

$$H_B=E_0+\sum_{\alpha\beta}\varepsilon_{\alpha\beta}b^+_\alpha b_\beta+\frac{1}{2}\sum_{\alpha\beta\gamma\delta}u_{\alpha\beta\gamma\delta}b^+_\alpha b^+_\beta b_\delta b_\nu, \tag{3.18}$$

where E_0 is a c-number, $\varepsilon_{\alpha\beta}$ and $u_{\alpha\beta\gamma\delta}$ are free parameters, and b^+_α and b_α are, respectively, creation and destruction (s or d) boson operators. The distinguishing property of this boson Hamiltonian is that it contains in addition to the harmonic term a two-body part and commutes with the total number of bosons. Moreover, it has a definite group structure, since the bilinear products are the 36 generators of the group $U(6)$. This allows us to find the proper basis states for its diagonalization. In fact, one can generate from $U(6)$ three subgroup chains containing the rotation group as a subgroup. These are

$$\begin{array}{llr} & U(5)\supset 0(5)\supset 0(3)\supset 0(2) & \mathrm{I}\\ & \nearrow & \\ U(6)\supset & \rightarrow SU(3)\supset 0(3)\supset 0(2) & \mathrm{II}\\ & \searrow & \\ & 0(6)\supset 0(3)\supset 0(2)\,. & \mathrm{III}\end{array} \tag{3.19}$$

Each group chain provides the quantum number for labeling a set of basis states.

The boson Hamiltonian, in its general form, can be diagonalized in one of these bases only numerically. For an appropriate choice of the parameters, however, it can be written as a sum of linear and quadratic Casimir invariants of one of the three chains. In these limiting cases the eigenvalue problem can be solved algebraically.

The states obtained in these three limits can be interpreted geometrically by making use of the concept of coherent states. It can be shown that in chain I the states describe the vibrational motions of spherical nuclei; chain II corresponds to an axially symmetric rotor, and chain III to a γ-unstable rotor.

In the second version of the interacting-boson model (IBM2) one makes the distinction between neutrons and protons and assumes that the low-lying levels of nuclei can be explained in terms of pairs of protons and pairs of neutrons with $J^\pi=0^+$ and $J^\pi=2^+$, treated as $s_\pi d_\pi$ and $s_\nu d_\nu$ bosons.

In order to take into account the $p-h$ conjugation in particle space, the number of protons, N_π, and the number of neutrons, N_ν, are counted from the nearest closed shell.

The Hamiltonian for the coupled system of proton and neutron bosons can be written as

$$H=H_\pi+H_\nu+V_{\pi\nu}, \tag{3.20}$$

where H_π (H_ν) is the proton (neutron) boson Hamiltonian of the form (3.18), and $V_{\pi\nu}$ is the proton–neutron boson interaction. The IBM2 also has a group structure, that of the group product $U_\pi(6)\otimes U_\nu(6)$. One can generate from this group several group chains containing the rotation group as a subgroup, each one leading to a definite classical limit.

The chain leading to the scissors mode is the following:

$$\begin{aligned}&U_\pi(6)\otimes U_\nu(6)\supset U_{(\pi+\nu)}(6)\\ &\quad\supset SU_{(\pi+\nu)}(3)\supset 0(3)\supset 0(2).\end{aligned} \tag{3.21}$$

Since the proton and neutron bosons are nonidentical, from the tensor product of the two $U(6)$ symmetric representations one generates symmetric as well as mixed-symmetry representations. In order to label the states of different $U_{\pi+\nu}(6)$ symmetry, it has become customary to introduce a new quantum number, called the F-spin, formally equivalent to isospin for particles. A proton boson has $F=1/2$ and third component $F_3=+1/2$, while a neutron boson has $F=1/2$ and $F_3=-1/2$. For a system of $N=N_\pi+N_\nu$ bosons, the totally symmetric states have maximum F-spin, $F=F_{mx}=(N_\pi+N_\nu)/2$, the states with mixed symmetry have $F=F_{mx}-1$, etc.

The most general IBM2 Hamiltonian has too many parameters to be of any practical use. A schematic Hamiltonian frequently used is of the form

$$\begin{aligned}H=&\,\varepsilon(n_{d\pi}+n_{d\nu})+2K_{\pi\nu}Q_\nu\cdot Q_\pi+K_{\nu\nu}Q_\nu\cdot Q_\nu\\ &+K_{\pi\pi}Q_\pi\cdot Q_\pi+\lambda M,\end{aligned} \tag{3.22}$$

where $n_{d\pi}$ and $n_{d\nu}$ are proton and neutron $J^\pi=2^+$ number operators, Q_π and Q_ν are the proton and neutron quadrupole operators, and M is the so-called Majorana operator, related to the Casimir invariant of the group $U_{\pi+\nu}(6)$ and responsible for the splitting between totally symmetric and mixed-symmetry representations.

In the special case $\varepsilon=0$ and $K_{\pi\nu}=K_{\pi\pi}=K_{\nu\nu}=K$ the Hamiltonian (3.22) can be expressed as the sum of the Casimir invariants of the group chain (3.21) and is therefore diagonal in this scheme. The energy spectrum can be calculated algebraically. One obtains symmetric as well as mixed-symmetry bands, where $J^\pi=1^+$ levels appear.

The first excited $J^\pi=1^+$ state describes the scissors mode.[4] Owing to the lack of experimental information on other mixed-symmetry levels, the Majorana parameter is fixed by fitting the observed energy of this $J^\pi=1^+$ state. The IBM cannot therefore predict the energy of the scissors mode.

The M1 operator has the form

$$\mathscr{M}(M1)=\sqrt{\frac{3}{4\pi}}(g_\pi L_\pi+g_\nu L_\nu)\mu_N=\mathscr{M}_s+\mathscr{M}_v, \tag{3.23}$$

where the F-spin scalar and vector components are

$$\mathscr{M}_s(M1,\mu)=\sqrt{\frac{3}{4\pi}}g_R L_\mu \mu_N=\sqrt{\frac{3}{4\pi}}g_R(L_{\pi,\mu}+L_{\nu,\mu})\mu_N, \tag{3.24}$$

$$\mathscr{M}_v(M1,\mu)=\sqrt{\frac{3}{4\pi}}(g_\pi-g_\nu)\left(\frac{N_\nu}{N}L_{\pi,\mu}-\frac{N_\pi}{N}L_{\nu,\mu}\right)\mu_N, \tag{3.25}$$

and the gyromagnetic factor is obtained from the F-spin scalar term

$$g_R=\frac{\langle\mu\rangle}{L}=\frac{g_\pi\langle L_\pi\rangle+g_\nu\langle L_\nu\rangle}{\langle L\rangle}=\frac{g_\pi N_\pi+g_\nu N_\nu}{N}. \tag{3.26}$$

The g_π and g_ν factors can be computed microscopically by following a boson–fermion mapping procedure.[146] Since the underlying idea in the IBM is that the s and d bosons represent strongly correlated $J^\pi=0^+$ and $J^\pi=2^+$ nucleon pairs, one can turn the boson state Ψ_B into a fermion state Ψ_F by replacing the boson operators s^+ and d^+ by correlated fermion pair operators

$$S^+=\sum_i c_i^{(0)}(a_i^+a_i^+)_0^0,\quad D_\mu^+=\sum_{ij} c_{ij}^{(2)}(a_i^+a_j^+)_\mu^2. \tag{3.27}$$

The boson operator O_B is then defined by equating the matrix elements,

$$\langle\Psi_B|O_B|\Psi_B'\rangle=\langle\Psi_F|O_F|\Psi_F'\rangle, \tag{3.28}$$

where O_F is the shell-model operator.

The microscopic estimates based on the above procedure give[147,148] $g_\pi\cong 1$ and $g_\nu\cong 0$. Alternatively, they can be estimated empirically from a comparison with the experimental g factor of the 2^+ states.[29,149,150] The values so determined can deviate from $g_\pi\cong 1$ and $g_\nu\cong 0$ by 25–30%.

The F-spin vector term couples the ground state to the $J^\pi=1^+$ mixed-symmetry state of the scissors mode with a strength given by[4,29,148]

$$B(M1)=\frac{3}{4\pi}\frac{8N_\pi N_\nu}{2N-1}(g_\pi-g_\nu)^2\mu_N^2. \tag{3.29}$$

It is to be noticed that only valence nucleons contribute to the strength. Using the values $g_\pi=1$ and $g_\nu=0$ for ^{156}Gd, $N_\pi=7$ and $N_\nu=5$, one obtains $B(M1)\cong 2.8\mu_N^2$, a value remarkably close to experiment.

The IBM form factor is computed by using the microscopic expression for the s and d bosons. It therefore contains some spin contribution. Its agreement with experiment is satisfactory even at high momentum transfers, where the spin term is dominant and where the TRM clearly appears to be inadequate.[107,108] These results have been confirmed in subsequent calculations.[151,152]

The IBM description of the mode is, on the other hand, closely related to the TRM. As we will see, in the classical limit the IBM Hamiltonian indeed assumes the TRM form.

The M3 operator has a similar structure:

$$\mathscr{M}(\mathrm{M3})=\sqrt{\frac{35}{8\pi}}(g_\pi^{(3)}(d_\pi^+d_\pi)_{3\nu}+g_\nu^{(3)}(d_\nu^+d_\nu)_{3\nu}), \tag{3.30}$$

where, in the absence of experimental data, the gyromagnetic ratios are determined microscopically by a boson–fermion mapping procedure similar to the one outlined for the M1 case. The model predicts[24] three M3 transitions, one F-spin symmetric transition, and two transitions of mixed symmetry, including the scissors mode. Numerically,[24,29] the mixed-symmetry transition strengths were found to be quite strong $[B(\mathrm{M3})\uparrow\simeq 0.35-0.6\mu_N^2b^2]$, while the symmetric strength turned out to be too weak $[B(\mathrm{M3})\uparrow\simeq 0.09\mu_N^2b^2]$ in comparison with the experimental value[142] $[B(\mathrm{M3})\uparrow\simeq 0.3\mu_N^2b^2]$.

2. Connection with the TRM and deformation law

The M1 strength given by Eq. (3.29) is valid in the $SU(3)$ limit. The most general IBM2 summed M1 strength consistent with the conservation of F-spin symmetry is[84]

$$B(\mathrm{M1})\uparrow=\frac{3}{16\pi}\langle 0|S^2|0\rangle(g_\pi-g_\nu)^2\mu_N^2 \simeq\frac{9}{4\pi}P\frac{\langle N_d\rangle}{N-1}(g_\pi-g_\nu)^2\mu_N^2, \tag{3.31}$$

where N_π and N_ν denote the numbers of valence proton and neutron pairs, respectively, $N=N_\pi+N_\nu$, $\langle N_d\rangle$ is the average number of quadrupole bosons in the ground state, and P the fractional number introduced by Casten:[153]

$$P=2\frac{N_\pi N_\nu}{N}. \tag{3.32}$$

The IBM2 M1 strength in the $SU(3)$ limit is obtained as a special case by putting $n_d=\langle N_d\rangle/N=2/3$.

One can derive a semiclassical expression for the IBM2 strength by the following procedure.[92] Let us write

$$N_d=N_d^{(p)}+N_d^{(n)}=d_p^\dagger\cdot d_p+d_n^\dagger\cdot d_n, \tag{3.33}$$

where $d_\tau^\dagger$ and d_τ denote the quadrupole boson creation and annihilation operators, respectively. Being a scalar, N_d can be referred to the intrinsic frame. In the classical limit, the

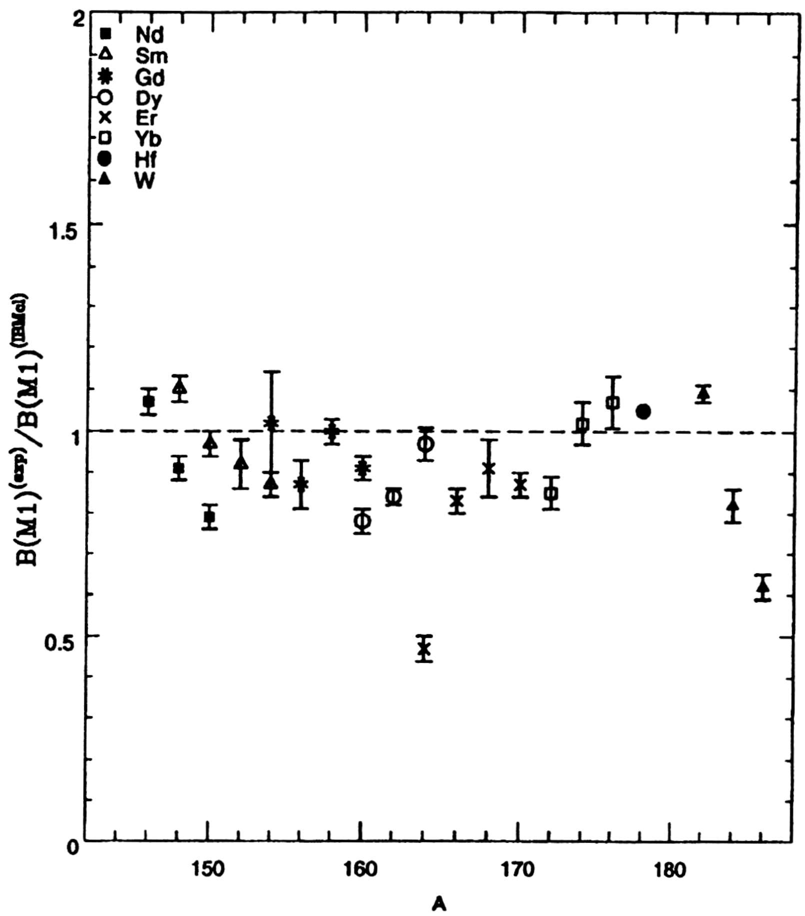

FIG. 2. Ratio between the IBM M1 strength computed in the semiclassical limit [Eq. (3.38)] and the experimental value in the rare-earth region.

harmonic approximation holds. We can then transform to shape variables by means of the canonical transformation

$$\alpha_{2\mu}^{(\tau)}=\alpha_0^{(\tau)}(d_{\tau,\mu}^{\dagger}+d_{\tau,\mu}),\quad \alpha_0^{(\tau)}=\sqrt{\frac{1}{2B_\tau\omega}}. \tag{3.34}$$

The $\mu=1$ components are the shape scissors variables. We can therefore take ω to be the energy of the scissors mode.

In dealing with an axially symmetric system it is appropriate to take as the intrinsic ground state a HO wave function which is coherent only in the proton and neutron $\mu=0$ components of $\alpha_{2\mu}^{(\tau)}$. We have

$$\begin{aligned} &d_{\tau,0}\psi_c=d'_\tau\psi_c,\\ &d_{\tau,\mu}\psi_c=0\quad(\mu\neq 0), \end{aligned} \tag{3.35}$$

where d'_τ are pure c-numbers. It follows that

$$\beta_\tau=\langle\alpha_{20}^{(\tau)}\rangle_c=2\alpha_0^{(\tau)}d'_\tau. \tag{3.36}$$

In the strong-coupling limit we then obtain

$$\begin{aligned}\langle N_d\rangle&=\frac{1}{4}\left[\left(\frac{\beta_p}{\alpha_0^{(p)}}\right)^2+\left(\frac{\beta_n}{\alpha_0^{(n)}}\right)^2\right]=\frac{1}{2}\,\omega(B_p\beta_p^2+B_n\beta_n^2)\\ &\simeq\frac{1}{2}\,\omega B\beta^2.\end{aligned} \tag{3.37}$$

This equation shows that the number of quadrupole bosons in the IBM2 ground state is strictly correlated with the Bohr–Mottelson deformation parameter β. The link between the M1 strength and the deformation is equally close. Indeed, upon insertion in Eq. (3.31) we get

$$B^{(\mathrm{cl})}(\mathrm{M1})\uparrow\simeq\frac{9}{8\pi}\frac{P}{N-1}\,\omega B\beta^2(g_\pi-g_\nu)^2\mu_N^2. \tag{3.38}$$

By virtue of this relation, the IBM2 strength appears to be quadratic in the deformation parameter, in accord with experiment. Such a property is hidden when the same strength is expressed in the IBM2 formalism. Figure 2 shows that in the classical limit of the IBM2 the experimental trend of the M1 strength is closely reproduced. Another method for deriving the classical limit of the same IBM M1 strength (3.31) has been developed in Ref. 91. The results are of the same quality.

3. The TRM as the geometric limit of the IBM2: explicit derivation

The close link between the IBM2 approach and the TRM was explicitly proved in Refs. 154–157. Using coherent states of the form

$$|\Psi_\alpha\rangle=\exp\left(\sum_{k=\pi,\nu}(\alpha_{sk}s_k^{+}+\alpha_{dk}\cdot d_k^{+})\right)|0\rangle, \tag{3.39}$$

the IBM Hamiltonian becomes a classical one:

$$H(\alpha_{sk},\alpha_k,\alpha_{sk}^*,\alpha_k^*)=\langle\Psi_\alpha|H_B|\Psi_\alpha\rangle,\quad k=p,n. \tag{3.40}$$

Because of the conservation of the total number of bosons N, α_{sk} can be expressed in terms of N and α_k. The resulting Hamiltonian depends on ten coordinates α_p and α_n, five for protons and five for neutrons, and their complex conjugates, as in the two boson models illustrated previously.

The link of the IBM, as well as of the other boson model, with the TRM can be established by the following procedure.

One can transform these shape coordinates α_k into the intrinsic coordinates β_k and γ_k and the Euler angles $(\alpha\beta\gamma)$ by the canonical transformation

$$\alpha_{k,\mu}=\sum_{\nu} a_{k,\nu}D^{(2)}_{\mu\nu}(\Omega_k), \tag{3.41}$$

and similarly for the conjugate momenta π_k. In this equation the $a_{k,\mu}$ are given by the expressions

$$a_{k,0}=\beta_k \cos\gamma_k,$$
$$a_{k,\pm 2}=\frac{1}{\sqrt{2}}\beta_k \sin\gamma_k, \tag{3.42}$$
$$a_{k,\pm 1}=0.$$

In the IBM the deformation parameter γ is equal to the corresponding Bohr and Mottelson quantity, while the parameter β is a function of the parameter β of Bohr and Mottelson.

In order to derive the Hamiltonian describing the scissors mode, one must freeze the shape variables by taking their equilibrium values. For an axially symmetric system one has $\gamma_\pi=\gamma_\nu=0$, while the values of β are obtained by minimizing the energy. Of the two sets of Euler angles ($\Omega=\alpha\beta\gamma$), the angles γ are redundant if we impose the condition $L_3^\pi=L_3^\nu=0$ consistently with the assumption of axial symmetry. The remaining angles can be transformed to an angle θ between the symmetry axes and to a set of Euler angles describing the orientation of the full system, exactly as in the TRM. This program was carried out explicitly, for instance, in Ref. 154. The starting point was an IBM2 Hamiltonian of the form

$$H_B=E_0+\varepsilon_d(n_{d\pi}+n_{d\nu})+KQ_\pi\cdot Q_\nu+\lambda M. \tag{3.43}$$

After having followed the above prescriptions, by making an expansion in θ and keeping the quadratic terms in the angular momenta $L_{k,\mu}$ the authors obtained, to lowest order in the $1/N$ expansion, apart from a constant,

$$H=\sum_{k=\pi,\nu}\frac{1}{\mathfrak{J}_k}(\rho_{k2}^2+\rho_{k2}^2)+\frac{1}{\mathfrak{J}_{\pi\nu}}\rho_\pi\cdot\rho_\nu+\frac{1}{2}C\theta^2, \tag{3.44}$$

where $\rho_{k\mu}=(1/N_k)L_{k\mu}$. The inertial parameters $\mathfrak{J}_k$ and $\mathfrak{J}_{\pi\nu}$ and the restoring-force constant are complicated functions of N_k, β_k, and the other parameters entering into the starting Hamiltonian.

The classical Hamiltonian (3.44) is formally identical to the TRM Hamiltonian (2.3). The only difference is the presence of the coupling term $L_\pi\cdot L_\nu$, which in the TRM appears only for $N\neq Z$.

One can therefore requantize the Hamiltonian by following the TRM procedure and obtain, as in the TRM, a two-dimensional HO Hamiltonian in θ. The excitation energy ω of the mode is now given by

$$\omega=\frac{4}{N}\left[C\left(\frac{2}{\mathfrak{J}_k}-\frac{1}{\mathfrak{J}_{\pi\nu}}\right)\right]^{1/2}. \tag{3.45}$$

The moment of inertia and the restoring-force constant are estimated using standard IBM parameters. Taking the average value $1/\mathfrak{J}=1/\mathfrak{J}_\pi+1/\mathfrak{J}_\nu$, one obtains for ^{156}Gd the value ω=2.96 MeV, which is a good approximation to the observed value ω=3.1 MeV.

We have already pointed out that the IBM and TRM form factors practically coincide up to moderate values of the momentum transfer. The IBM is more successful at higher momenta. The success of the IBM over the semiclassical description is generally attributed to the fact that in the IBM the neutron–proton rotational oscillation is executed by valence nucleons only. In order to check this point, it was assumed in the TRM that only the part of the proton and neutron fluids external to an inert core takes part in the motion.[158] Such a change, however, spoils the agreement of the TRM with the experimental form factor. The success of the IBM description is rather to be ascribed to dynamical correlations which, among other things, allow, though effectively, for spin contributions. In particular, the rather satisfactory agreement of the M1 IBM form factor with experiment at high q values is due to the spin degrees of freedom, which are effective only at high momentum transfer.

Though accounting well for the collective properties of the M1 mode, the IBM2, like all other phenomenological approaches, cannot account for the M1 strength distribution. Attempts to explain the fragmentation of the strength by including additional bosons[25,28] or by changing the parameters of the Majorana force[159] were clearly inadequate.

4. MICROSCOPIC DESCRIPTIONS: SHELL-MODEL CALCULATIONS

All boson descriptions are based on the quantization of the quadrupole shape variables α_p and α_n and lead in the geometric limit to a semiclassical description formally equivalent to the one provided by the TRM.

However, important differences appear between the same boson descriptions when these are in quantized form. This is to be expected, since the Hamiltonians and the methods used to handle the eigenvalue problem differ from model to model. In particular, a major difference between the IBM and the other two models can be noticed. While in fact the IBM is a boson number-conserving scheme, the other two approaches are not.

The microscopic implications of such a difference are of great importance. The IBM bosons, as we saw, can be considered to lowest order as highly correlated valence nucleon pairs. The bosons in the NPD and the GCS models are instead to be viewed to lowest order as highly correlated $p-h$ nucleon states. The IBM can indeed be considered as a truncated shell-model scheme in which the valence nucleons are so strongly pairwise correlated that they allow a description in terms of bosons. The microscopic counterpart of the NPD and CGSM is to lowest order the random-phase approximation (RPA) scheme.

The microscopic descriptions of the scissors mode indeed fall into these two major schemes, the standard shell model and the RPA. The shell model has been adopted to study M1 excitations only in light and medium-light nuclei. In heavy nuclei, calculations of this kind are prohibitive because of the exceedingly large dimensions of the configuration space. Only shell-model calculations with a group-theoretical basis and relying on severe approximations have been carried out for heavy nuclei.

A. Shell-model approaches in light nuclei

Zamick[39–41] has shown that M1 states with a strength of about 1 μ_N^2 can be generated in the restricted $f_{7/2}^n$ shell-model space. These states have the form

$$\Psi_J=\sum_{L_pL_n v} D_J(L_pL_n v)[(f_{7/2}^2)_{L_p}\otimes(f_{7/2}^n)_{L_n}]^J, \tag{4.1}$$

where v is the seniority quantum number, and D_J is the probability amplitude for two protons, coupled to angular momentum L_p, and n neutrons, coupled to angular momentum L_n, to couple to total spin J.

The M1 operator induces a transition from the $J^\pi=0^+$ ground state to the $J^\pi=1^+$ excited states with a strength

$$\begin{aligned}B(M1,\ 0^+\rightarrow 1^+)&=|\langle\Psi_{1^+}\|\mathscr{M}(M1)\|\Psi_{0^+}\rangle|^2\\&=(3/4\pi)\mu_N^2(g_p-g_n)^2\\&\quad\times\left|\sum_{Lv} D_0(LLv)D_1(LLv)\sqrt{L(L+1)}\right|^2,\end{aligned} \tag{4.2}$$

where the proton and neutron gyromagnetic factors are the effective ones appropriate for a single j shell:

$$g=\frac{l}{j}g_l+\frac{g_s}{2j}. \tag{4.3}$$

Using the orthogonality relation

$$\sum_\alpha D_{J\alpha}(LL)D_{J\alpha}(L'L')=\delta_{LL'}, \tag{4.4}$$

it is straightforward to obtain the integrated strength

$$\sum_\alpha B^\alpha(\mathrm{M1},0^+\rightarrow 1_\alpha^+)=(3/4\pi)\mu_N^2(g_p-g_n)^2\sum_L |D_0(LL)|^2L(L+1). \tag{4.5}$$

The appearance of the factor (g_p-g_n) stresses the isovector character of the transitions. The scissors nature can be proved by rendering explicit the link with the TRM. Indeed,

$$\sum_L |D_0(LL)|^2L(L+1)=\langle\Psi_0|J_p^2|\Psi_0\rangle=\frac{1}{4}\langle\Psi_0|S^2|\Psi_0\rangle=\frac{1}{4}\Im\omega. \tag{4.6}$$

We then obtain the standard TRM expression (2.11). In this case, however, the strength receives a contribution from both the orbital and the spin components. This is due to the fact that the calculation is carried out within a single j shell, so that the M1 operator takes the form (2.63) with effective gyromagnetic ratios (4.3). Similar expressions have been derived for the strengths of magnetic transitions of higher multipolarity ($\lambda=3,5,7$).

Numerical calculations have been performed for Ti isotopes, using a nucleon–nucleon interaction determined empirically from the observed levels of ^{42}Sc under the assumption that these ^{42}Sc states are due to the configuration $(1f_{7/2})^2$. The numerical results show that the M1 transition strength is mostly concentrated in the lowest $J^\pi=1^+$ state. The strengths of the transitions of higher multipolarity are instead strongly fragmented and have a spin contribution which increases with the multipolarity, a result also found by Heyde and Sau.[160]

The schematic shell model underestimates the orbital (with respect to the spin) contribution to the M1 strength. For ^{46}Ti the calculated ratio is $R=\sqrt{B_l}/\sqrt{B_l}\simeq 0.86$, while the observed ratio is $R\simeq 3.5$. If configuration mixing with a higher shell is included,[161,162] the ratio increases to $R\simeq 2.5$. The calculation reproduces nicely the M1 and M3 form factors.

Studies of the M1 mode in Ti isotopes have been carried out with satisfactory (and, in many ways, similar) results also in the RPA.[71]

B. $SU(3)$ shell model

It has already been pointed out that the M1 mode is excited through the operator

$$S_+=L_+^{(p)}-L_+^{(n)}. \tag{4.7}$$

If we confine ourselves to a major shell and use a HO basis, the $L_+^{(\tau)}$ can be viewed as the generators of the $SU_\tau(3)$ groups. The connection with this group can be made more transparent by observing that

$$S_+|0\rangle=-(8\pi/15)^{1/2}m(\omega_1+\omega_3)\sum_n |K^\pi=1^+,n\rangle\langle K^\pi=1^+n|Q_{+1}|0\rangle, \tag{4.8}$$

where

$$Q=r_p^2Y_{2,1}(r_p)-r_n^2Y_{2,1}(r_n). \tag{4.9}$$

Namely, $L_+^{(\tau)}$ acts just like the quadrupole operators $Q_{+1}^{(\tau)}$, which are also generators of $SU_\tau(3)$.

In the $SU(3)$ model[163] the Hamiltonian is composed of a HO one-body term H_0 plus a quadrupole–quadrupole $(Q-Q)$ two-body potential. For a given major shell this interaction represents the leading term in the expansion of any long-range Wigner interaction. Its use is therefore justified in the LS coupling limit. This is the case for light nuclei. For these nuclei, isospin is also a good quantum number. The states must therefore belong to the antisymmetric representation of the group $SU(3)\otimes SU_{\sigma\tau}(4)$. Being the orbital space of a major shell of degeneracy s, the states with a given symmetry can be classified according to the irreducible representations of $U(s)$, $U(3)$, and $SO(3)$. If the spin–isospin components are characterized by S and T, the basis states can be written

$$|\Psi_\alpha\rangle = |[f](\lambda\mu)KLMST\rangle, \tag{4.10}$$

where $[f]$ and $(\lambda\mu)$ label the $U(s)$ and $U(3)$ representations, respectively, KLM are the rotational quantum numbers, and S and T label the spin and isospin wave function. The scissors states are obtained by acting with the scissors operator S_+ on the ground state. In ^{20}Ne, for instance, the M1 state is

$$\begin{aligned} |1^+T=1\rangle &= S_+|[4](80)K=0,\ L=J=0,\ S=0,\ T=0\rangle \\ &= |[31](61)K=1,\ L=1,\ S=0,\ T=1\rangle. \end{aligned} \tag{4.11}$$

It is worth noting that the generator S_+ transforms the completely symmetric (antisymmetric) orbital (spin–isospin) part into one of mixed symmetry. In other nuclei with $T\neq 0$, like ^{22}Ne, S_+ generates more than one scissors state.

A shell-model $SU(3)$ study of M1 excitations in light nuclei of the *sd* shell, like ^{20}Ne, ^{22}Ne, and ^{36}Ar, and of the *pf* shell, like ^{44}Ti, was carried out by Poves *et al.*[45–47] The findings of their calculation were as follows:

(i) The integrated M1 strength of all $J^\pi = 1^+$ states is $\Sigma B(\mathrm{M1}) = 2.43\mu_N^2$ in ^{20}Ne and $\Sigma B(\mathrm{M1}) = 3.60\mu_N^2$ in ^{36}Ar.

(ii) In ^{20}Ne, 75% of the strength is concentrated in the lowest $J^\pi = 1^+$ state at $\omega \simeq 11$ MeV and comes mostly from the convection current.

(iii) In ^{36}Ar the strength is shared mainly by four $J^\pi = 1^+$ states. The difference between the M1 distribution in the well deformed ^{20}Ne and that in the vibrational ^{36}Ar can be interpreted as a confirmation of the peculiarity of the scissors mode, whose existence is closely related to deformation according to the TRM and the schematic RPA.

In heavy nuclei the $SU(3)$ symmetry is spoiled by the strong spin–orbit coupling term. This causes a large separation between the members of the Nilsson spin–orbit doublets and pushes the state of maximum j down to the next lower major shell. As a result, a major shell is composed of a set of normal-parity orbits and one abnormal-parity s.p. state.

One can observe, however, that the states of a given N shell with $l-1/2$ and $(l-2)+1/2$ are very close in energy.[164–166] Exploiting the fact that the normal-parity states of a given shell have the same total angular momenta as the levels of an oscillator shell with $N = N-1$, one can make the mapping $N \to N-1$, $l-1/2 \to l+1/2 = (l-1)+1/2$, $(l-2)+1/2 \to (l-1)-1/2$.

After relabeling the Nilsson states with pseudo-oscillator quantum numbers $[\tilde{N}\tilde{n}\tilde{\Lambda}\tilde{\Omega}]$, the members of the new spin–orbit doublet with $\tilde{\Omega} = \tilde{\Lambda} \pm 1/2$ appear very close in energy. The normal-parity states can therefore be classified according to a pseudo-$SU(3)$.[167,168] Such a scheme can work only under the assumptions that (i) particles in the abnormal-parity single j shell are dominated by the pairing interaction, so that the dominant configurations arising from this shell are zero-seniority states with $J_\pi^A = J_\nu^A = 0$; (ii) the interaction between normal- and abnormal-parity states is weak; (iii) proton and neutron spatial wave functions in the normal-parity space are totally symmetric, so that $\tilde{S}_\pi = \tilde{S}_\nu = 0$. Under these assumptions, the nuclear state is of the form[48,49]

$$\Psi_{JM} = (\Psi_{JM}^N \otimes \Psi_{JA}^A)_{JM}, \tag{4.12}$$

where the completely antisymmetric normal-parity (Ψ_{JM}^N) and abnormal-parity (Ψ_{JA}^A) states are, respectively, classified according to the chains

$$\begin{aligned} &U(\Omega_N^\sigma) \to U(\Omega_{N/2}) \otimes U(2) \to SU(3) \otimes SU(2) \to O(3) \\ &\qquad \otimes SU(2) \to SU(2), \\ &U(\Omega_A^\sigma) \to S_p(\Omega_A^\sigma) \to O(3), \end{aligned} \tag{4.13}$$

where Ω_N and Ω_A are the dimensions of the two groups and S_p is the compact symplectic group. Because of the pseudospin s.p. basis and the assumptions made, the magnetic-dipole operator $\mathcal{M}(\mathrm{M1})$ is purely orbital:

$$\mathcal{M}(\mathrm{M1}) = \tfrac{1}{2}(g_\pi + g_\nu)\tilde{L} + \tfrac{1}{2}(g_\pi - g_\nu)(\tilde{L}_\pi - \tilde{L}_\nu). \tag{4.14}$$

The theory predicts from one to four $J^\pi = 1^+$ states, the actual number depending on the leading $SU(3)$ proton and neutron irreducible representations. For completely symmetric proton and neutron $SU(3)$ representations $(\lambda_\pi, 0) \times (\lambda_\nu, 0)$, as in ^{154}Sm and ^{238}U, there is only one $J^\pi = 1^+$ state. For such a state the M1 transition strength is given by

$$B(\mathrm{M1},\ J^\pi = 0 \to 1^+) = 364\pi(g_\pi - g_\nu)^2 \frac{2\lambda_\pi\lambda_\nu}{(\lambda_\pi + \lambda_\nu - 1)}, \tag{4.15}$$

which has the same structure as in the IBM2 expression (3.29), with λ_τ replacing N_τ.

When only one π (or ν) irreducible representation is symmetric, as in ^{156}Gd, there are two $J^\pi = 1^+$ states, both collective. In general, as in ^{164}Dy or ^{168}Er, neither the $SU_\pi(3)$ nor the $SU_\nu(3)$ ones are symmetric. In this case there are four $J^\pi = 1^+$ states, three of them corresponding to $K^\pi = 1^+$ bands, and the other belonging to a $K^\pi = 0^+$ band. Only two of the three $J^\pi = 1^+$ states have large M1 strength, while the state belonging to the $K^\pi = 0^+$ band is moderately collective.

Aside from the M1 strengths, the authors have also calculated the magnetic moments μ, which fixed the gyromagnetic factors ($g_\pi = 1$ and $g_\nu = 0$), as well as the branching ratio $B(\mathrm{M1},\ 1^+ \to 2^+)/B(\mathrm{M1},\ 1^+ \to 0^+)$, which supports the axial symmetry of the nuclei under study. The calculations underestimate the M1 strength by about a factor of two.

5. RPA DESCRIPTIONS

Most of the experimental analyses have been devoted to the search for and characterization of the mode in heavy nuclei, especially of the rare-earth region. The main feature of the mode in these nuclei is the fragmentation of the M1 strength. None of the phenomenological or schematic approaches discussed previously can account for such a property. Full shell-model studies would be needed. They are not feasible, however, for heavy nuclei. One must therefore rely on approximations. The RPA has been the approximation scheme adopted most extensively.

A. RPA general formalism

In the RPA the nuclear eigenvalue problem is formally converted into a HO eigenvalue equation.[169,170] For this purpose one defines the eigenstates of the nuclear Hamiltonian as

$$|\lambda\rangle = O_\lambda^+|0\rangle, \tag{5.1}$$

where the operators O_λ^+ are such that its Hermitian conjugates satisfy the equation

$$O_\lambda|0\rangle = 0. \tag{5.2}$$

This last equation defines the nuclear ground state $|0\rangle$ as the vacuum for the operators O_λ and O_λ^+. Such a vacuum is in general a highly correlated state. Because of the above assumptions the eigenvalue equation can be written in the HO form

$$[H,O_\lambda^+]|0\rangle = \omega_\lambda O_\lambda^+|0\rangle = (E_\lambda - E_0)O_\lambda^+|0\rangle. \tag{5.3}$$

The RPA consists in solving these equations in a restricted $p-h$ space, so that the operator O_λ^+ is of the form

$$O_\lambda^+ = \sum (Y_{ph}^\lambda a_p^+ a_h - Z_{ph}^\lambda a_h^+ a_p). \tag{5.4}$$

The states $|\lambda\rangle$ are normalized according to

$$\delta_{\lambda\lambda'} = \langle\lambda|\lambda'\rangle = \langle 0|O_\lambda O_{\lambda'}^+|0\rangle = \langle 0|[O_\lambda, O_{\lambda'}^+]|0\rangle \cong \langle|[O_\lambda, O_{\lambda'}^+]|\rangle, \tag{5.5}$$

where $|\rangle$ is the $p-h$ vacuum. The last approximate equality expresses the quasiboson approximation. By virtue of this approximation, the normalization condition yields

$$\sum_{ph} (Y_{ph}^{\lambda *} Y_{ph}^{\lambda'} - Z_{ph}^{\lambda *} Z_{ph}^{\lambda'}) = \delta_{\lambda\lambda'}. \tag{5.6}$$

The RPA eigenvalue equations are

$$\begin{vmatrix} A & B \\ B^* & A^* \end{vmatrix} \begin{vmatrix} Y_\lambda \\ Z_\lambda \end{vmatrix} = h\omega_\lambda \begin{vmatrix} Y_\lambda \\ -Z_\lambda \end{vmatrix}, \tag{5.7}$$

where

$$\begin{aligned} A_{ph,p'h'} &= \langle|[a_h^\dagger a_p, [H, a_{p'}^\dagger a_{h'}]]|\rangle = (\varepsilon_p - \varepsilon_h)\delta_{pp'}\delta_{hh'} + V_{ph'h'p}, \\ B_{ph,p'h'} &= -\langle|[a_p^\dagger a_h, [H, a_{h'}^\dagger a_{p'}]]|\rangle = V_{pp'hh}. \end{aligned} \tag{5.8}$$

The transition amplitudes for the generic one-body operator W are given by

$$\langle\lambda|W|0\rangle = \langle 0|[O_\lambda, W]|0 \cong \langle|[O_\lambda, W]|\rangle = \sum_{ph} (Y_{ph}^{\lambda *} W_{ph} + Z_{ph}^{\lambda *} W_{hp}). \tag{5.9}$$

In the QRPA the states have the form

$$|\lambda\rangle = O_\lambda^\dagger|0\rangle = \sum \{Y_{\alpha\beta}^\lambda \alpha_\alpha^\dagger \alpha_\beta^\dagger - Z_{\alpha\beta}^\lambda \alpha_\beta \alpha_\alpha\}|0\rangle, \tag{5.10}$$

where $\alpha_\alpha^\dagger$ (α_α) are creation (destruction) quasiparticle operators defined by the Bogoliubov transformation

$$\begin{aligned} \alpha_\alpha^\dagger &= u_\alpha a_\alpha^\dagger - v_\alpha a_{\bar\alpha}, \\ u_\alpha^2 &+ v_\alpha^2 = 1. \end{aligned} \tag{5.11}$$

The QRPA eigenvalues are still obtained by solving Eqs. (5.7) with the matrix elements

$$\begin{aligned} A_{\alpha\beta,\gamma\delta} &= \langle 0|[\alpha_\beta\alpha_\alpha, [H, \alpha_\gamma^\dagger\alpha_\delta^\dagger]]|0\rangle \cong (E_\alpha + E_\beta)\delta_{\alpha\gamma}\delta_{\beta\delta} + \tilde{V}_{\alpha\beta\gamma\delta}, \\ B_{\alpha\beta,\gamma\delta} &\simeq \langle 0|[\alpha_\beta\alpha_\alpha, [H, \alpha_\delta\alpha_\gamma]]|0\rangle \cong \tilde{V}'_{\alpha\beta\gamma\delta}, \end{aligned} \tag{5.12}$$

where E_α is the quasiparticle energy and $|0\rangle$ is now the quasiparticle vacuum. We omit the explicit expressions for $\tilde{V}_{\alpha\beta\gamma\delta}$ and $\tilde{V}'_{\alpha\beta\gamma\delta}$, which are rather involved and can be found, for instance, in Ref. 169.

The QRPA transition amplitudes for the generic operator W are given by

$$\langle\lambda|W|0\rangle \simeq \langle 0|[O_\lambda, W]|0\rangle = \sum_{\alpha>\beta} (Y_{\alpha\beta}^{\lambda *} W_{\alpha\beta} + Z_{\alpha\beta}^{\lambda *} W_{\beta\alpha}) \times (u_\alpha v_\beta + \tau v_\alpha u_\beta), \tag{5.13}$$

where $\tau = +1$ or -1 according as the operator W is even or odd under time reversal.

The eigenvalues and the transition amplitudes can be determined only numerically, using a proper s.p. deformed basis. In the BCS approach only the coefficients u_α and v_α are determined self-consistently by using the pairing force only, while the s.p. basis is determined independently. In the Hartree–Bogoliubov (H.B.) method both the s.p. states and the u_α and v_α coefficients are determined self-consistently from a unique interaction.

B. RPA Hamiltonians

The first studies of the mode have been carried out in the schematic RPA.[34–37] As already pointed out, their results coincide with those derived in Sec. 2.D for the TRM. We will therefore not report on them. We mention only that a schematic calculation which accounts also for spin admixtures was carried out to compute the M3 transition.[171] The results were close to those derived for the TRM.[106]

Apart from a few calculations using a Skyrme interaction[55] or a Landau–Migdal force,[59,67,68] most of the realistic studies have been carried out using a separable interaction either in the RPA (Refs. 52–54, 56–58, 60–66, and 69–77) or in the Tamm–Dancoff approximation.[78,79]

A guide for guessing which multipoles should enter into the interaction is provided by phenomenological and schematic models. From their analysis we can infer that an RPA Hamiltonian should contain at least the following terms:

$$H = H_0 + V_{P-P} + V_{Q-Q} + V_{\sigma\sigma}. \tag{5.14}$$

The first term is a one-body deformed Hamiltonian

$$H_0 = \sum_i h_i = \sum_i (T_i + V_i), \tag{5.15}$$

where T_i is the nucleon kinetic term and V_i is the nucleon deformed potential. This is either of the Nilsson[78] or the Woods–Saxon form (for instance, Refs. 53 and 60). The

$p-h$ energy spectrum produced by the one-body potential is extremely fragmented with intermixed orbital and spin excitations.[172,173]

The second part is the monopole and quadrupole pairing for protons and neutrons,

$$V_{P-P}=\sum_{k=p,n}[G_0^{(k)}P_0^{(k)\dagger}P_0^{(k)}+G_2^kP_2^{(k)\dagger}P_2^{(k)}], \tag{5.16}$$

where

$$P_J^\dagger=\sum_{\alpha,\beta}[a_\alpha^\dagger\otimes a_\beta^\dagger]_J. \tag{5.17}$$

The third part is the $Q-Q$ interaction, which in the isospin formalism is

$$V_{Q-Q}=1/2\sum_{T=0,1}\chi_Q(T)[Q(T)Q^\dagger(T)+Q^\dagger(T)Q(T)], \tag{5.18}$$

where

$$Q\left(T=\begin{matrix}0\\1\end{matrix}\right)=Q_{+1}^{(p)}\pm Q_{+1}^{(n)}. \tag{5.19}$$

Finally, we have the spin–spin interaction

$$V_{\sigma\sigma}=1/2\sum_{T=0,1}\chi_\sigma(T)[\sigma(T)\sigma^\dagger(T)+\sigma^\dagger(T)\sigma(T)], \tag{5.20}$$

where

$$\sigma\left(T=\begin{matrix}0\\1\end{matrix}\right)=s_{+1}^{(p)}\pm s_{+1}^{(n)}. \tag{5.21}$$

The importance of the $Q-Q$ and monopole pairing interactions becomes clear from the microscopic analysis of the TRM or, what amounts to the same thing, from schematic RPA calculations (Sec. 2.D). As shown there, the quadrupole fields are closely related to the proton and neutron angular momenta. They enter directly in the M1 $p-h$ channel. Monopole pairing qualifies the rotors as superfluids and has the effect of quenching the M1 strength without spoiling the scissors picture. The necessity of the quadrupole pairing can be inferred from the fact that the $L=2$ correlated valence pairs are the building blocks of the IBM states. The major role played by such a term emerges explicitly from displaying the structure of the schematic SM wave function:[39]

$$\begin{aligned}\Psi_0&=D_0(L_p=0,\ L_n=0)|0\rangle+D_0(L_p=2,\ L_n=2)|(2_p\\&\quad\otimes 2_n)_0\rangle,\\ \Psi_1&=D_1(L_p=2,\ L_n=2)|(2_p\otimes 2_n)_1\rangle.\end{aligned} \tag{5.22}$$

The M1 transition is clearly due to the $L=2$ correlations among like valence nucleons. Monopole and quadrupole pairing have the effect of redistributing the $p-h$ M1 spectrum by inducing a concentration of scissors excitation around 3 MeV.[172,173] The role of quadrupole pairing in the RPA was studied in Ref. 70. The spin–spin term is dictated by the spin–orbit admixtures in the s.p. states and by the large number of low-energy $p-h$ spin excitations intermixed with the orbital ones. Because of its repulsive character, the spin–spin interaction has the important effect of pushing up in energy the spin excitations, which become separated from the M1 orbital transitions, in accord with experiment and with the scissors picture.[78]

Although all the terms included in Eq. (5.14) play a major role, we cannot rule out the possibility that other parts of the nuclear Hamiltonian not present in Eq. (5.14) may affect the M1 channel. It has been stressed, for instance, that the so-called recoil term reduces the fragmentation of the two-quasiparticle spectrum, thereby concentrating the strength around a main peak, in accord with experiment, and enforces the scissors nature of the transitions.[174–176]

C. Spurious rotational admixtures

The study of the mode in a realistic RPA approach has encountered a series of problems.[177] A major one was the occurrence of spurious rotational admixtures, pointed out for the first time in Ref. 60. Since the RPA eigenvalue problem is formulated in the intrinsic system, the RPA ground state breaks the spherical symmetry, so that

$$J_{+1}|0\rangle\neq 0. \tag{5.23}$$

This state separates out at zero energy from the other RPA states if the starting Hamiltonian is rotationally invariant. In this case, in fact, we have

$$(H-E_0)J_{+1}|0\rangle=[H,J_{+1}]|0\rangle=0. \tag{5.24}$$

Namely, $J_{+1}|\rangle$ is an exact eigenstate with zero eigenvalue. It is therefore automatically orthogonal to the other RPA states.

The Hamiltonian used in almost all calculations, however, is not rotationally invariant, so that

$$\langle K^\pi=1^+|J_{+1}|0\rangle\neq 0. \tag{5.25}$$

Several techniques have been developed to remove the rotational state. The first one[60] consists in adding a symmetry-restoring term to the Hamiltonian:

$$H\rightarrow H'=H-\sum \nu\lambda_\nu J_-O_\nu^+(K^\pi=1^+), \tag{5.26}$$

where the Lagrange multipliers λ_ν are determined by the constraint

$$\langle K^\pi=1^+,\nu|J_+|0\rangle=\langle 0|O_\nu(K^\pi=1^+)J_+|0\rangle=0. \tag{5.27}$$

Since such a condition depends upon the solution, the RPA equations become nonlinear, so that their final determination requires an iterative procedure.

A second procedure, adopted in the TDA,[78] consists in using the Schmidt orthogonalization procedure on the two-quasiparticle states. These have the form

$$|\alpha_1\alpha_2\rangle=|\alpha_1\alpha_2\rangle_{sp}-J_+|0\rangle\langle 0|J_-|\alpha_1\alpha_2\rangle_{sp}. \tag{5.28}$$

The states so constructed are no longer eigenstates of the starting unperturbed Hamiltonian, so that an iterative procedure is needed also in this case.

A third procedure, adopted in Ref. 72, consists in using the Pyatov prescription[178] of replacing the quadrupole field in the Hamiltonian by

$$F_1^{(\tau)}=[H_0,J_+^{(\tau)}]. \tag{5.29}$$

The condition of rotational invariance

$$[H,J_+]=0 \tag{5.30}$$

imposes on the fields F the following constraint:

$$\begin{aligned}&1+k_{pp}\langle[F_1^{(p)\dagger},J_+^{(p)}]\rangle+k_{nn}\langle[F_1^{(n)\dagger},J_+^{(n)}]\rangle=0,\\&1+k_{nn}\langle[F_1^{(n)\dagger},J_+^{(n)}]\rangle+k_{pp}\langle[F_1^{(p)\dagger},J_+^{(p)}]\rangle=0.\end{aligned} \tag{5.31}$$

In other approaches[77] the problem is avoided by using a j-projected s.p. basis, which makes it possible to formulate the problem directly in the laboratory frame. Finally, the separation can be achieved by using a self-consistent basis. This has been done in Ref. 61, and partly in Ref. 55. The problem can be clearly illustrated in the schematic RPA.[179]

D. Self-consistent fields and rotational admixtures: a simple approach

Let us assume[179] that Z protons and N neutrons move in a spherical HO mean field with frequency ω_0 and interact through a $Q-Q$ force. The Hamiltonian therefore has the rotationally invariant form

$$\begin{aligned}H=H_0&+\frac{1}{2}\chi\sum_\mu\,(Q_{2\mu}^{(p)*}Q_{2\mu}^{(p)}+Q_{2\mu}^{(n)*}Q_{2\mu}^{(n)})\\&+\frac{1}{2}\chi_{pn}\sum_\mu\,(Q_{2\mu}^{(p)*}Q_{2\mu}^{(n)}+Q_{2\mu}^{(n)*}Q_{2\mu}^{(p)}),\end{aligned} \tag{5.32}$$

where

$$Q_{2\mu}^{(\tau)}=\sum_i q_{2\mu}^{(\tau)}(i)=\sum_i r_i^{(\tau)}Y_{2\mu}^{(\tau)}(i). \tag{5.33}$$

1. Self-consistent mean field and doubly stretched coordinates

In the Hartree approximation we obtain, for the ith proton or neutron deformed mean field,

$$V_H^{(\tau)}=\frac{1}{2}m\omega_0^2r^2-\beta_\tau m\omega_0^2q_{20}^{(\tau)}, \tag{5.34}$$

having defined

$$\begin{aligned}&\chi\langle Q_{20}^{(p)}\rangle+\chi_{pn}\langle Q_{20}^{(n)}\rangle=-\beta_p m\omega_0^2,\\&\chi\langle Q_{20}^{(n)}\rangle+\chi_{pn}\langle Q_{20}^{(p)}\rangle=-\beta_n m\omega_0^2.\end{aligned} \tag{5.35}$$

The Hartree potential can be written in the form of an anisotropic HO potential

$$V^{(\tau)}=\frac{1}{2}m\omega_1^2(\tau)(x_1^{(\tau)^2}+x_2^{(\tau)^2})+\frac{1}{2}m\omega_3^2(\tau)x_3^{(\tau)^2} \tag{5.36}$$

with frequencies

$$\begin{aligned}&\omega_1(\tau)=\omega_0\sqrt{1+\frac{2}{3}\delta_\tau}\simeq\omega_0\left(1+\frac{1}{3}\delta_\tau\right),\\&\omega_3(\tau)=\omega_0\sqrt{1-\frac{4}{3}\delta_\tau}\simeq\omega_0\left(1-\frac{2}{3}\delta_\tau\right),\end{aligned} \tag{5.37}$$

where $\delta_\tau=\sqrt{45/(16\pi)}\beta_\tau$. The same potential can be put in the "spherical" form

$$V^{(\tau)}=\frac{1}{2}m\omega_0^2(\tilde{x}_1^{(\tau)^2}+\tilde{x}_2^{(\tau)^2}+\tilde{x}_3^{(\tau)^2}) \tag{5.38}$$

if we use doubly stretched coordinates[180–183] $\tilde{x}_i=(\omega_i/\omega_0)x_i$. These are to be used in the quadrupole operator entering into the $Q-Q$ Hamiltonian so as to preserve its spherical character. This transformation indeed ensures that the Hartree field is not further distorted once the interaction is switched on. We have, in fact,

$$\langle\tilde{Q}_{20}^{(p)}\rangle=\langle\tilde{Q}_{20}^{(n)}\rangle=0 \tag{5.39}$$

if we impose the conditions

$$\omega_1^{(\tau)}\sum_1^\tau=\omega_2^{(\tau)}\sum_2^\tau=\omega_3^{(\tau)}\sum_3^\tau, \tag{5.40}$$

where $\Sigma_i^\tau=\Sigma_i^\tau(n_i+1/2)$. The explicit form of the $\tilde{Q}$ operators is

$$\begin{aligned}&\tilde{Q}_{\pm1}=\frac{\omega_1\omega_3}{\omega_0^2}Q_{\pm1},\\&\tilde{Q}_{\pm2}=\frac{\omega_1^2}{\omega_0^2}Q_{\pm2},\\&\tilde{Q}_{\pm0}=\frac{1}{3\omega_0^2}(\omega_1^2+2\omega_3^2)Q_0-\frac{\sqrt{5}}{3\omega_0^2}(\omega_1^2-\omega_3^2)r^2Y_{00}.\end{aligned} \tag{5.41}$$

Since the doubly stretched quadrupole operator also contains a monopole term, the new $Q-Q$ potential is composed of pure quadrupole–quadrupole plus monopole–quadrupole and monopole–monopole terms.

The Hartree conditions fix the isoscalar coupling constant. Summing the two equations in (5.34) and making use of standard formulas for the quadrupole moments, we obtain, to lowest order in δ, the well known result[133]

$$\chi(0)=\frac{1}{2}(\chi+\chi_{pn})\simeq-\frac{4\pi}{5}\frac{m\omega_0^2}{A\langle r^2\rangle}. \tag{5.42}$$

The isovector coupling constant $\chi(1)$ can be derived from the symmetry-energy mass formula[133] and turns out to be related to $\chi(0)$ by the ratio $b=-\chi(1)/\chi(0)\simeq3.6$. According to some analyses,[75,184] however, this value is too large.

A quasiparticle RPA calculation formulated in the $\Delta N=0+2$ space has been carried out.[179] It was shown that, by virtue of the self-consistent conditions (5.35), the schematic quasiparticle RPA gives a vanishing root. This is the eigenvalue of the redundant rotational mode. Such a state turns out to be completely removed from the intrinsic ones. Indeed, one obtains

$$\langle n,K^\pi=1^+|L_+|0\rangle\propto P(x)=x^3+ax^2+bx+c=0, \tag{5.43}$$

where $P(x)=P(\omega^2)=0$ is the eigenvalue equation giving the roots of the M1 physical states.

This method of removing the spurious rotational state, though developed within the schematic RPA, has a more general validity. Indeed, the Hartree conditions (5.35) can be written in the form

$$1+k_{pp}\langle[F_1^{(p)\dagger},J_+^{(p)}]\rangle+k_{nn}\langle[F_1^{(n)\dagger},J_+^{(n)}]\rangle=0, \tag{5.44}$$

$$1+k_{nn}\langle[F_1^{(n)^\dagger},J_+^{(n)}]\rangle+k_{pp}\langle[F_1^{(p)^\dagger},J_+^{(p)}]\rangle=0,$$

where

$$F_1^{(\tau)}=[H_0,J_+^{(\tau)}]. \tag{5.45}$$

These constitute precisely the Pyatov ansatz (5.31) for removing the rotational mode. They are therefore valid for any one-body potential and any separable Hamiltonian.

2. Scissors sum rule in the RPA

It has already been pointed out that for the scissors mode the energy-weighted M1 sum rule is given by Eq. (2.66). This quantity has been computed in phenomenological domains such as the IBM2,[79,86–88] in the spherical shell model,[42] and in a schematic approach using a deformed mean field (no interaction).[81] Recently, the same sum rule has been computed in the RPA.[185] For this purpose a separable interaction which includes a $Q-Q$ interaction with doubly stretched coordinates has been adopted. The final result was

$$S_{\mathrm{EW}}^{(\mathrm{sc})}(\mathrm{M1})=\frac{3}{16\pi}(S_1^{(\mathrm{sc})}+S_{20}^{(\mathrm{sc})}+S_{22}^{(\mathrm{sc})})g_r^2\mu_N^2. \tag{5.46}$$

The first term comes from the Hartree field and is given by

$$S_1^{(\mathrm{sc})}=\frac{1}{2}\sum_{\mu=\pm1}\langle 0|[S_\mu^\dagger,[H_0,S_\mu]]|0\rangle=3m\omega_0^2(\beta_p\langle Q_{20}^{(p)}\rangle+\beta_n\langle Q_{20}^{(n)}\rangle), \tag{5.47}$$

which is what was obtained in Ref. 81, where only a deformed mean field was considered. The second part comes from the two-body interaction involving the monopole operators and is given by

$$S_2^{(0)}=-3m\omega_0^2(\beta_p\langle Q_{20}^{(p)}\rangle+\beta_n\langle Q_{20}^{(n)}\rangle). \tag{5.48}$$

It is equal and opposite to the one-body contribution (5.47), which therefore cancels. Therefore the only remaining contribution is from the pure $Q-Q$ potential, apart from modifications induced by the use of stretched coordinates. This is given to lowest order in δ by

$$S_{\mathrm{EW}}^{(\mathrm{sc})}(\mathrm{M1})\simeq-\frac{9}{4\pi}\chi_{pn}\left(\sum_n B_n^{(0)}(E2)\uparrow-\sum_n B_n^{(1)}(\mathrm{E2})\uparrow\right), \tag{5.49}$$

which is the result obtained in the spherical shell model.[42] Stretched coordinates are responsible for higher-order terms, which, however, are not negligible.[185] Experimentally, the E2 strength to the lowest 2^+ state is orders of magnitude larger than the strengths of the other transitions. If these are ignored, one obtains

$$\omega^{(-)}B(\mathrm{M1})^{(-)}+\omega^{(+)}B(\mathrm{M1})^{(+)}\simeq-\frac{9}{4\pi}\chi_{pn}\times B_0^{(0)}(\mathrm{E2})\uparrow. \tag{5.50}$$

It follows that

$$B(\mathrm{M1})^{(\pm)}\propto B_0^{(0)}(\mathrm{E2})\uparrow\propto\delta^2. \tag{5.51}$$

The sum-rule approach presented here gives a quite general theoretical proof of the quadratic deformation law holding for the M1 strengths of both low-lying and high-energy scissors modes.

E. Realistic RPA calculations

The earlier RPA calculations produced contradictory results. Some of them had seriously questioned the scissors nature of the mode.[53,54,59] The reason for these discordances can be easily explained. The M1 channel is extremely sensitive to the s.p. energies, to the kind of interaction used, and, for a given interaction, to the choice of the strengths of the different separable pieces. As already pointed out,[177] these early approaches used different and incomplete Hamiltonians and relied on several untested approximations. Moreover, the M1 states produced by these calculations were contaminated with spurious rotational admixtures. Most of the recent studies are free of most of these limitations and, consequently, tend to converge to similar results.

The goal of RPA calculations can be summarized in the following points. They should (i) account for the collective properties of the mode, such as the quadratic deformation dependence of the total M1 strength; (ii) exhibit the microscopic structure of the M1 states, so as to enable one to decide about the scissors nature of the mode; (iii) reproduce closely the energy distribution of the M1 strength.

Concerning the first point, calculations carried out by different groups have reproduced fairly well the deformation law.[69,74,77,79] The crucial role of pairing correlation in enforcing such a law was particularly stressed. As clearly illustrated in Fig. 3, the agreement with experiment would be almost perfect if the spin contribution could be suppressed.[74,79] Indeed, such good agreement was reached in Ref. 77, where the spin contribution was effectively suppressed by the j-projected basis. In this basis, in fact, deformation is taken into account only perturbatively. The necessity of spin suppression dictated by the experimental data supports implicitly the scissors picture. Such a picture is tested more explicitly by computing the summed overlap

$$\sum_n|\langle K^+,n|\psi_{\mathrm{sc}}\rangle|^2, \tag{5.52}$$

where $|\psi_{\mathrm{sc}}\rangle$ is the scissors state defined as

$$|\psi_{\mathrm{sc}}\rangle=\alpha J_+^{(p)}|0\rangle+\beta J_+^{(n)}|0\rangle. \tag{5.53}$$

The coefficients are determined by imposing its normalization to unity and its orthogonality to the rotational state:

$$\langle\psi_{\mathrm{sc}}|\psi_{\mathrm{sc}}\rangle=1,\quad\langle\psi_{\mathrm{sc}}|J_+|0\rangle=0. \tag{5.54}$$

The summed overlap for the states below 4 MeV is found to be about 40%, a very large number in view of the fact that, as discussed in Sec. 2.D, the model predicts another scissors state at high energy.[177] This latter mode is predicted also by realistic RPA calculations.[59,68,72,76] Its degree of fragmentation, however, is not settled. It seems[186] that if the two-quasiparticle space is truncated up to 30 MeV, the mode is

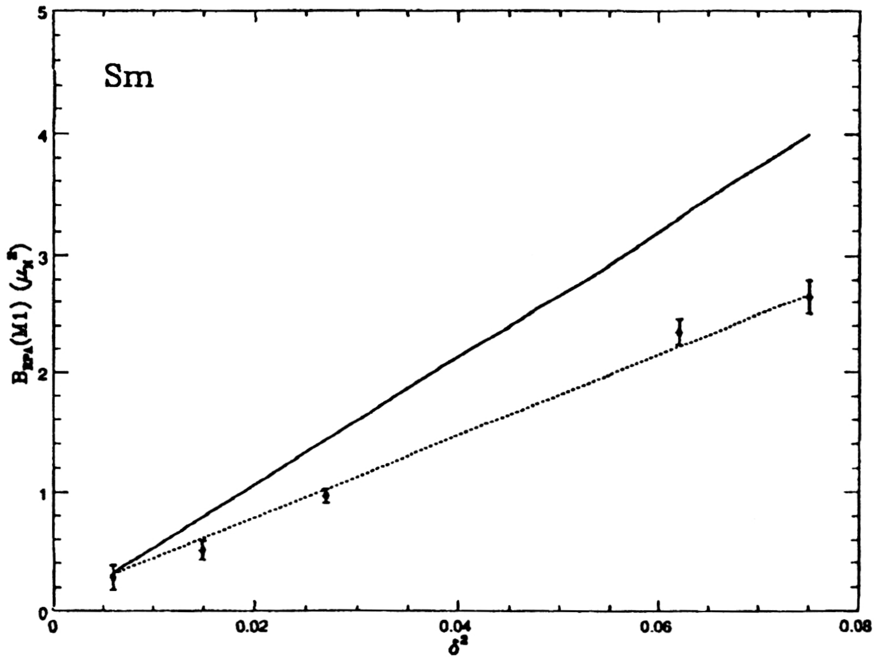

FIG. 3. Deformation dependence of the M1 strength computed in the RPA versus experiment. The dotted line gives the orbital contribution.

basically not fragmented, in agreement with the schematic picture.[177] It becomes strongly fragmented if the two-quasiparticle space is enlarged.

As we said, the systematic experimental study of the scissors mode has led to the other interesting discovery of spin excitations.[21,22] These have been detected in ^{154}Sm and ^{156}Gd in the energy range 5–11 MeV and have a very peculiar property. The profile of the spectrum exhibits two distinct bumps. These transitions have been studied with good success in the TDA (Refs. 187 and 188) as well as in the RPA (Refs. 67, 68, 70, 74 and 77). There is, however, no conclusive interpretation of the observed two-peak structure. It is indeed not clear whether the two peaks correspond to different proton and neutron excitations[70,77,187,188] or are of isovector and isoscalar nature.[74] The calculations which support the first picture use a vanishing coupling constant for the isovector spin–spin interaction. The supporters of the other interpretation use a nonvanishing value. In the first case, deformation plays an important role; in the second case, it is not relevant. This fact suggests that the issue can be settled by a systematic analysis which covers both spherical and deformed nuclei.

RPA calculations have been carried out to describe the M1 excitations not only in rare-earth nuclei, but also in actinides,[66,73] in medium-light nuclei,[71] and in medium nuclei.[63] On the whole, the results are satisfactory. An unsolved problem remains, however. The energy distribution of the M1 strength is not well reproduced. This suggests that maybe the RPA space should be enlarged so as to allow for higher configurations.

6. BEYOND THE RPA: THE QPNM APPROACH

Notably, TDA and RPA calculations are carried out in a $p-h$ or two-quasiparticle space. On energetic grounds, however, higher-order configurations can also contribute to the mode. Many four-quasiparticle excitations fall within or just above the energy range where the low-lying M1 transitions are observed. In order to study the effect of these states, it is necessary to enlarge the space. This has been achieved within the QPNM.[93] In this approach[94] the nuclear system is studied in a space spanned by one plus two RPA phonon states. Most of the properties of all nonrotational states up to 2.5 MeV in deformed nuclei, including all Eλ and Mλ transitions, have been studied in this scheme.[189–196]

A. Brief description of the QPNM

The starting QPNM Hamiltonian has the following structure:

$$H=H_{\text{s.p.}}+H_{\text{pair}}+H_M+H_S+H_T. \tag{6.1}$$

The first term is the one-body Hamiltonian, which includes a deformed axially symmetric Saxon–Woods potential, the second is a proton (neutron) monopole pairing interaction, and the other three are isoscalar and isovector spin-independent (H_M), spin-dependent (H_S), and tensor (H_T) two-body interactions. All these terms are written in separable form. The two-body interaction acts in the $p-h$ as well as in the particle–particle ($p-p$) channels. The $p-p$ component of the spin-independent part yields also a quadrupole pairing term, which adds to the monopole pairing interaction. One may notice that the QPNM Hamiltonian is considerably more complex than those adopted in the RPA.

The first step of the QPNM is to make use of the Bogoliubov canonical transformation and to express the Hamiltonian in terms of quasiparticle operators $\alpha_{q\sigma}$ and $\alpha^\dagger_{q\sigma}$. The symbols $q\sigma$ stand for the s.p. asymptotic quantum numbers $q\sigma=Nn_z\Lambda\uparrow$ for $K^\pi=\Lambda+1/2$ and $q\sigma=Nn_z\Lambda\downarrow$ for $K^\pi=\Lambda-1/2$. RPA phonons are then constructed:

$$Q^\dagger_{Kn\sigma}=\frac{1}{2}\sum_{q_1q_2}\{\psi^{Kn}_{q_1q_2}A^\dagger_{K\sigma}(q_1q_2)-\phi^{Kn}_{q_1q_2}A_{K-\sigma}(q_1q_2)\}, \tag{6.2}$$

where $A^\dagger_{K\sigma}(q_1q_2)$ $[A_{K\sigma}(q_1q_2)]$ are pairs of creation (annihilation) quasiparticle operators. Their actual structure can be found in Ref. 194. Using the equations defining $Q^\dagger_{Kn\sigma}$ and $Q_{Kn\sigma}$, it is possible to bring the Hamiltonian (6.1) into the quasiparticle phonon form

$$H_{\mathrm{QPNM}}=H_q+H_v+H_{vq}, \tag{6.3}$$

where H_q and H_v are, respectively, the one-body quasiparticle and RPA phonon Hamiltonians, and H_{vq} is the quasiparticle phonon coupling term. The expressions for them can be found in Ref. 194.

Finally, the transformed Hamiltonian is put into diagonal form by using the variational principle with a trial wave function

$$\Psi_n(\sigma K^\pi=1^+)$$
$$=\left\{\sum_i R_i^n Q_v^\dagger+\frac{1}{2}m\sum_{v_1\sigma_1v_2\sigma_2} s^\sigma_{v_1\sigma_1v_2\sigma_2}\times P^n_{v_1v_2}Q^\dagger_{v_1\sigma_1}Q^\dagger_{v_2\sigma_2}\right\}\Psi_0, \tag{6.4}$$

where

$$s^\sigma_{v_1\sigma_1v_2\sigma_2}=\delta_{\sigma_1\mu_1+\sigma_2\mu_2,\sigma K}(1+\delta_{v_1,v_2})^{1/2}. \tag{6.5}$$

The labels v and v_k stand for the multipolarities of the RPA phonons, $v=(\lambda_0\mu_0)_i=(21)_i$ and $v_k=(\lambda\mu)_k$. The eigenvalues E_n are the roots of the secular equation

$$\det\|(\omega_v-E_n)\delta_{i,i'}-\sum_{v_1\geqslant v_2}\frac{\mathscr{C}(v_1v_2)U^v_{v_1v_2}U^{v'}_{v_1v_2}}{\omega_{v_1}+\omega_{v_2}+\Delta\omega(v_1v_2)+\Delta(v_1v_2)-E_n}\|=0, \tag{6.6}$$

where

$$\mathscr{C}(v_1v_2)=\frac{1+\mathscr{K}(v_1,v_2)}{1+\delta_{v_1,v_2}}. \tag{6.7}$$

The quantity ω_v denotes the RPA energies, $U^v_{v_1v_2}$ describes the coupling between one- and two-phonon states, and $\mathscr{K}$ is a term introduced to take fully into account the Pauli principle in the two-phonon components of the total wave function [Eq. (6.4)]. This term induces the energy shift $\Delta\omega(v_1v_2)$ in the eigenvalue equation. The other energy shift $\Delta(v_1v_2)$ is due to the coupling to three-phonon states not included explicitly in the calculation. Its value is approximately $\Delta(v_1v_2)\simeq-0.2\Delta\omega(v_1v_2)$.

B. Calculations and results

Numerical calculations have been carried out for a chain of Gd and Dy isotopes. Single-particle energies and wave functions were computed from the deformed axially symmetric Woods–Saxon potential by solving the eigenvalue problem in a space spanned by quasiparticle plus quasiparticle RPA phonon states for each odd nucleus. The calculation, whose details can be found in Refs. 94, 194, 196, and 197, is then iterated until good agreement with the experimental data is reached. Such a procedure fixes the parameters of the potential as well as the quadrupole and hexadecapole deformation parameters β_2 and β_4. The values of all the parameters can be found in Refs. 93 and 197. The s.p. spectrum was taken from the bottom of the well up to +5 MeV.

Two-quasiparticle configurations up to an excitation energy of 30 MeV were taken into account. Monopole and quadrupole pairing were included in the calculation of the quasiparticle energies and amplitudes. The quadrupole pairing was extracted from the $\lambda\mu=20$ $p-p$ interaction. This term plays an important role in determining the properties of the 0^+ states in deformed nuclei.[198] For a fixed value of its strength G^{20}, the strength of the monopole pairing was determined so as to reproduce the experimental odd–even mass differences. The blocking effect and the Gallagher–Moszkowski corrections[199] were taken into account in computing the two-quasiparticle energies.

The separable interaction includes spin-dependent and spin-independent $p-h$ multipole terms. The strengths of the spin-independent isoscalar $p-h$ interaction terms $\kappa_0^{\lambda\mu}$ were fixed so as to reproduce the lowest experimental energy level for each $K^\pi\neq1^+$ (Refs. 194–196). The only parameters left were the isovector multipole constants and the spin strengths. The former were fixed according to the relation $\kappa_1^{\lambda\mu}=-1.5\kappa_0^{\lambda\mu}$, in substantial agreement with other choices.[60] The spin isoscalar coupling constant was taken to be ten times smaller than the isovector one, in accordance with the estimates obtained in a sum-rule description of spin excitations in heavy spherical nuclei.[200] All the parameters used in the study of the M1 modes can be found in Ref. 93. The only parameter left was the coupling constant of the isoscalar $\lambda\mu=21$ $Q-Q$ interaction. This was taken to be slightly larger than a critical value, for which the lowest RPA $K^\pi=1^+$ state vanishes. With this value the redundant rotational state turns out to be practically orthogonal to the other intrinsic states. Its overlap with each one of them is less than 0.005.

The basis consists of RPA phonons with $\lambda=2$–5 multipolarities. Twenty $\lambda\mu=21$ phonons and ten of the others were included. The $K^\pi=1^+$ RPA states were computed by including $p-h$ and $p-p$ isoscalar and isovector quadrupole and spin–spin interactions. The M1 strengths have been calculated by using a spin quenching factor $g_s=0.7$.

The M1 strength distributions obtained in the RPA and the QPNM for ^{158}Gd are shown in Fig. 4 for illustrative purposes.

From the figure and from a systematic analysis of the results one may draw the following general conclusions:

i) In each nucleus the RPA calculation yields a strong peak of the order of $(1-1.5)\mu_N^2$. Because of the coupling to the two-phonon space, this peak splits into two of weaker intensity.

ii) The fragmentation induced by the coupling is otherwise modest. It is appreciable only above 3 MeV. This reflects the fact that the coupling between one- and two-phonon states is weak.

iii) On the whole, the moderate increase in fragmentation improves the agreement with experiment. This can be improved by slight changes of properly chosen parameters. As shown in the figure, a change of the strength of the $\lambda\mu$

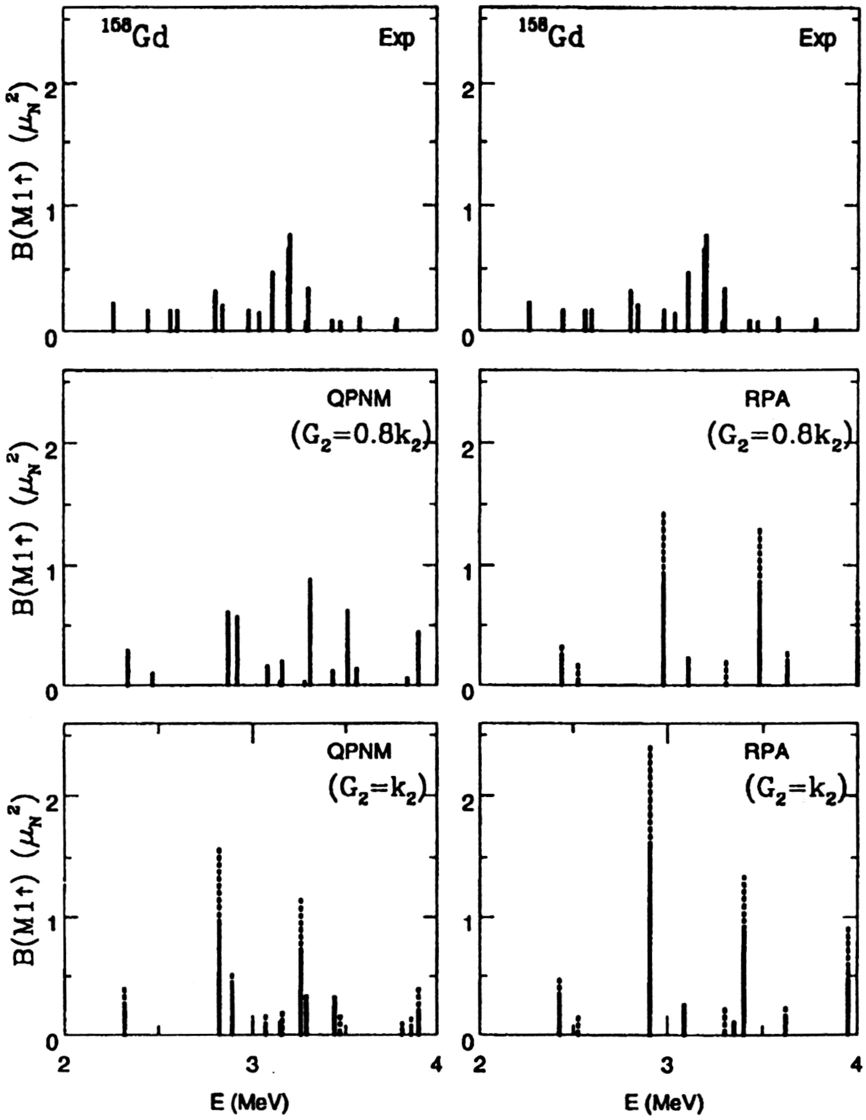

FIG. 4. QPNM and RPA M1 strength distributions in ^{158}Gd. The full part of each peak gives the orbital strength.

=21 $p-p$ (pairing) interaction produces sizable changes in the M1 spectrum.

iv) The nature of the transition is not modified by the coupling to the two-phonon states. Most of the strongly excited low-lying QPNM states are dominated by a single RPA phonon. In both RPA and QPNM calculations, practically all the transitions are of orbital nature. A modest spin admixture, however, affects considerably the intensity of the transition. In general, the spin contribution to the amplitude is additive.

v) The total overlap with the scissors state is 49% in the RPA and 45% in the QPNM. Most of the remaining percentage goes to the high-lying states.

vi) The theoretical summed M1 strength is larger than the one observed experimentally by a factor ~1.2–1.4, mainly because of the spin contribution.

vii) As in the RPA (see Fig. 3) the agreement with experiment would improve drastically if a mechanism leading to a partial suppression of the spin contribution could be found.

The QPNM was also adopted to study magnetic excitations with higher multipoles, in particular the M3 transitions.[191] It was found that the spin–octupole isovector interaction plays an important role and shifts the M3 strength up in energy into the region of the isovector magnetic resonances. The remaining M3 strength is fragmented and mainly of spin nature.

7. EXCITATIONS IN ODD-MASS DEFORMED NUCLEI

The question of whether the scissors mode survives as we move from even- to odd-mass nuclei was posed some time ago in studies carried out within the interacting boson–fermion model (IBFM),[95,96] in the schematic RPA,[97] and within the generalized coherent-state model (GCSM).[98]

After a first unsuccessful attempt,[99] dipole transitions which seem to have the properties of the scissors mode have been detected in several odd-mass deformed nuclei of the rare-earth region.[20,100,101] The first experimental search for M1 transitions in odd-mass nuclei was carried out in inelastic electron scattering on ^{165}Ho.[99] No strong M1 transition near 3 MeV was found in this nucleus.

Subsequent NRF experiments on ^{163}Dy have detected a sizable M1 strength around 3 MeV which, though more fragmented, fits nicely into the systematics of the scissors mode in the neighboring even–even Dy isotopes.[100] A concentration of dipole strength with the same properties has been found also in other rare-earth nuclei,[20] and more recently in ^{167}Er.[101] In this latter experiment, which covered a wider energy range, 1.9–4.3 MeV, peaks around and above 4 MeV have been detected. The interpretation of these excitations as a manifestation of a scissor-like oscillation mode found support in a theoretical analysis carried out within the IBFM.[100,101]

Though appealing, such a response cannot be considered conclusive. In the IBFM, in fact, as in all other schematic approaches,[97,98] the problem of fragmentation, which is of crucial importance in odd nuclei, is overlooked.

The theoretical study of M1 excitations in odd nuclei is rendered difficult not only by the extreme fragmentation of some of these spectra, but also by uncertainties inherent in the experimental analysis which will be discussed later. In fact, the polarization techniques, adopted for parity assignment in doubly even nuclei, are ineffective when applied to odd-mass nuclei. Because of this limitation, the presence of E1 excitations intermixed with M1 transitions cannot be ruled out. The schematic models are clearly inadequate for clarifying the nature of spectra of such complexity. One may hope to gain a more clarifying response from microscopic calculations. A fully microscopic calculation which accounts also for the coupling to two-phonon states has been carried out recently.[103]

A. With RPA core states

Equations for describing the nonrotational states in odd-mass deformed nuclei using RPA core states were derived in Ref. 201. These states have the form

$$\Psi_n^{\tau_0}(\sigma_0 K_0^{\pi_0})=\left\{\sum_{q_0}^{\tau_0} C_{q_0}^n \alpha_{q_0\sigma_0}^\dagger+\sum_{q_1\sigma_1}^{\tau_0}\sum_{v_2\sigma_2} \times \delta_{\sigma_1 K_1+\sigma_2\mu_2,\sigma_0 K_0} D_{q_1 v_2}^n \alpha_{q_1\sigma_1}^\dagger Q_{v_2\sigma_2}^\dagger\right\}\Psi_0, \tag{7.1}$$

with the normalization condition

$$\sum_{q_0}^{\tau_0}(C_{q_0}^n)^2+\sum_{q_1 v_2}^{\tau_0}(D_{q_1 v_2}^n)^2[1+\mathscr{L}^{K_0}(q_1;v_2)]=1. \tag{7.2}$$

Here the factor

$$\mathscr{L}^{K_0}(q_1;v_2)=-\sum_{q_2}(\psi_{q_1 q_2}^{v_2})^2 \tag{7.3}$$

comes from antisymmetrizing the quasiparticle–phonon components of (7.1). This was done for the first time in Ref. 202. Using the above wave function, one deduces energies and eigenvectors from the variational principle. They can be found in Ref. 94.

B. With QPNM core states

As was shown in Refs. 93, 195, and 203, at energies above 2.5 MeV the coupling to the two-phonon configurations induces fragmentation of the $K^\pi=1^+$ and $K^\pi=0^-,1^-$ modes in doubly even nuclei. Being interested in the distribution of the magnetic and electric transitions falling in the energy range 2.5–3.5 MeV, we need to take such a two-phonon coupling into account also in odd-mass nuclei. The mathematical procedure developed in Ref. 204 is followed. The basic idea is to use the already fragmented phonons in the wave functions of excited states according to the procedure described by Eqs. (4.86)–(4.90) in Ref. 94. For this purpose, the following trial wave function is chosen:

$$\Psi_n^{\tau_0}(\sigma_0 K_0^{\pi_0})=\Bigg[\sum_{q_0}^{\tau_0} C_{q_0}^n \alpha_{q_0\sigma_0}^\dagger+\sum_{q_1\sigma_1}^{\tau_0} \times \sum_{\substack{v_2\sigma_2\\ \lambda_2\mu_2\neq\bar{\lambda}\bar{\mu}}} \delta_{\sigma_1 K_1+\sigma_2\mu_2,\sigma_0 K_0} D_{q_1 v_2}^n \alpha_{q_1\sigma_1}^\dagger Q_{v_2\sigma_2}^\dagger + \sum_{q_3\sigma_3}^{\tau_0}\sum_{\bar{n}\bar{\sigma}} \delta_{\sigma_3 K_3+\bar{\sigma}\bar{\mu},\sigma_0 K_0} \bar{D}_{q_3\bar{\lambda}\bar{\mu}\bar{n}}^n \alpha_{q_3\sigma_3}^\dagger \Omega_{\bar{\lambda}\bar{\mu}\bar{n}\bar{\sigma}}^\dagger\Bigg] \times\Psi_0, \tag{7.4}$$

with the normalization condition

$$\sum_{q_0}^{\tau_0}(C_{q_0}^n)^2+\sum_{\substack{q_1 v_2\\ \lambda_2\mu_2\neq\bar{\lambda}\bar{\mu}}}^{\tau_0}(D_{q_1 v_2}^n)^2[1+\mathscr{L}^{K_0}(q_1;v_2)] +\sum_{q_3\bar{n}}^{\tau_0}(\bar{D}_{q_3\bar{\lambda}\bar{\mu}\bar{n}}^n)^2=1. \tag{7.5}$$

The QPNM core states have the quantum numbers $\{\bar{n}, \bar{\lambda}=2, \bar{\mu}=1\}$ for the M1 excitations and $\{\bar{n}, \bar{\lambda}=3, \bar{\mu}=0\}$ or $\{\bar{n}, \bar{\lambda}=3, \bar{\mu}=1\}$ for the $\Delta K=0$ or $\Delta K=1$ E1 transitions, respectively.

Under the assumption

$$[\alpha_{q\sigma},\Omega_{\bar{v}}^\dagger]=0, \tag{7.6}$$

which is a valid approximation when the energy of the core states is above 2.5 MeV, a variational calculation yields a secular equation whose rank is equal to the number of one-quasiparticle states of the wave function (7.4).

The E1 and M1 transition probabilities were computed by using the total wave function

$$\Psi_{nMK^\pi\sigma}^I=\sqrt{\frac{2I+1}{16\pi^2}}[D_{MK}^I\Psi_{nK^\pi\sigma} +(-1)^{I+K}D_{M-K}^I\Psi_{nK^\pi-\sigma}]. \tag{7.7}$$

For the reduced E1 transition probabilities an effective charge was taken:

$$e_{\rm eff}^{(1)}(\tau_z)=-\frac{e}{2}\left(\tau_2-\frac{N-Z}{A}\right)(1+\chi). \tag{7.8}$$

The factor χ is a fitting parameter introduced to quench the excessively large E1 transition probabilities obtained with the standard expression ($\chi=0$). For the M1 reduced strength

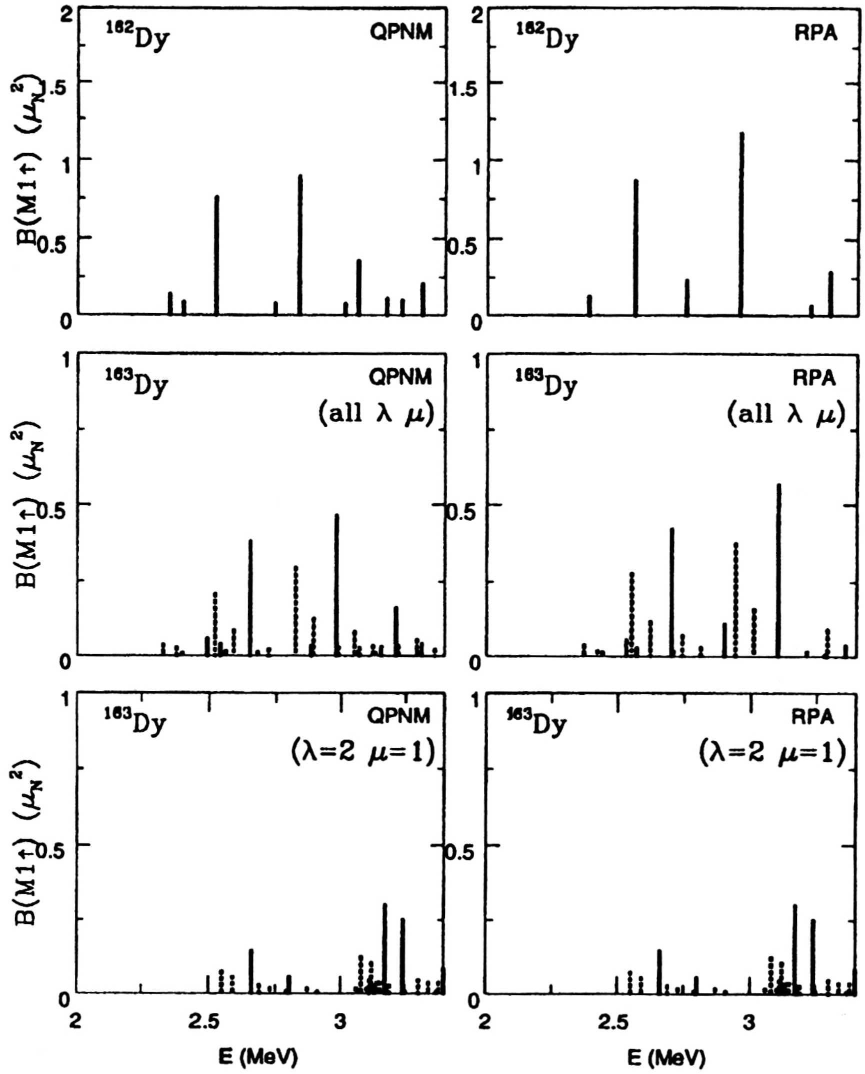

FIG. 5. QPNM and RPA M1 strength distributions in ^{162}Dy and ^{163}Dy. The full and dotted lines refer, respectively, to transitions to $K_f=3/2$ and $K_f=7/2$ final states.

a bare orbital gyromagnetic factor and an effective spin factor $g_s^{\mathrm{eff}}=0.7g_s^{\mathrm{free}}$ were used. Given the impossibility of distinguishing experimentally between E1 and M1 transitions in odd-mass nuclei, it is appropriate to compute the widths, multiplied by the statistical factor $g=(2I_f+1)/(2I_0+1)$. These quantities are in fact parity- and spin-independent, and are related to the reduced strengths according to

$$g\Gamma_0(\mathrm{E1})=1.0467(E_\gamma[\mathrm{MeV}])^3B(\mathrm{E1})\uparrow[e^2\mathrm{fm}^2 10^{-3}]\ \mathrm{meV},$$
$$g\Gamma_0(\mathrm{M1})=11.547(E_\gamma[\mathrm{MeV}])^3B(\mathrm{M1})\uparrow[\mu_N^2]\ \mathrm{meV}. \tag{7.9}$$

A more closely related quantity is represented by the reduced widths

$$g\Gamma_0^{\mathrm{red}}(\mathrm{E1})=1.0467B(\mathrm{E1})\uparrow[e^2\mathrm{fm}^2 10^{-3}]\ \mathrm{meV}(\mathrm{MeV})^{-3},$$
$$g\Gamma_0^{\mathrm{red}}(\mathrm{M1})=11.547B(\mathrm{M1})\uparrow[\mu_N^2]\ \mathrm{meV}(\mathrm{MeV})^{-3}. \tag{7.10}$$

The phonons of different multipolarity were calculated by using isoscalar and isovector interactions embodying the appropriate multipole fields. The phonon basis consists of ten ($i=1,2,\ldots,10$) phonons of a given multipolarity: $\lambda\mu=20$, 22, 32, 33, 43, 44, 54, 55. Twenty-five ($i=1,2,\ldots,25$) phonons of $\lambda\mu=21$ and $\lambda\mu=30$, 31 multipolarities were used. The same phonon basis was used for doubly even and odd-mass nuclei.

Numerical calculations were carried out for ^{157}Gd, ^{159}Tb, ^{161}Dy, ^{163}Dy, and ^{167}Er. The core states entering into the quasiparticle–phonon basis are, respectively, the states of ^{156}Gd, ^{158}Gd, ^{160}Dy, ^{162}Dy, and ^{166}Er.

1. M1 transitions

In going from even to odd nuclei, the fragmentation of the strength is dramatically enhanced. This phenomenon is illustrated in Fig. 5, showing the M1 spectra computed within the RPA and QPNM for ^{162}Dy and ^{163}Dy. The spectrum of the odd-mass nucleus is much richer than in the case of the doubly even one. A further increase in fragmentation is observed when the M1 core states are computed in the QPNM rather than in the RPA.

That the strength should become strongly fragmented in going from doubly even to odd-mass nuclei was largely expected. On the one hand, the quasiparticle$\otimes(\overline{\lambda\mu})_i$ components couple to several one-quasiparticle configurations. As a rule, the fragmentation so induced is rather weak, owing to the small number of one-quasiparticle states. On the other hand, the strength collected by each M1 state in a doubly even nucleus is distributed among four M1 levels in the neighboring odd-mass nucleus. In this latter system, in fact, the M1 operator can couple the $\{K_0, I_0=K_0\}$ ground state to a multiplet of four excited states with quantum numbers $\{(K_0-1, I_0-1), (K_0-1, I_0), (K_0-1, I_0+1)\}$, and $\{K_0+1, I_0+1\}$.

Let us study this problem more quantitatively by analyzing the results obtained for ^{163}Dy. The strength of the strongest M1 transition occurring in ^{162}Dy at an excitation energy $E=2.90$ MeV and estimated to be $B(\mathrm{M1})\uparrow \cong 0.90\mu_N^2$ is distributed in ^{163}Dy almost equally among the $K_f^\pi=3/2^-$ and $K_f^\pi=7/2^-$ levels, both having an intrinsic excitation energy of 2.89 MeV. The two K_f^π states indeed collect, respectively, as

$$\sum_{I_f^\pi} B(\mathrm{M1})\left(K_i^\pi=I_i^\pi=\frac{5^-}{2}\to K_f^\pi=\frac{3^-}{2}\,I_f^\pi\right)\simeq 0.45\mu_N^2,$$

$$B(\mathrm{M1})\left(K_i^\pi=I_i^\pi=\frac{5^-}{2}\to K_f^\pi=I_f^\pi=\frac{7^-}{2}\right)\simeq 0.47\mu_N^2.$$

The $K_f^\pi=3/2^-$ strength, however, is further distributed among the $I_f^\pi=3/2^-$, $5/2^-$, $7/2^-$ states with strengths $B(\mathrm{M1})\simeq 0.30$, 0.13, 0.02 μ_N^2, respectively. The $I_f^\pi=3/2^-$ state gets about 2/3 of the strength. That the $I_f^\pi=K_f^\pi$ states take 2/3 of the K_f^π strength is a general feature to be ascribed to angular-momentum coupling.

The states collecting appreciable amounts of M1 strength are dominated by a single quasiparticle–phonon configuration obtained by coupling the valence quasiparticle to the $(\bar{\lambda}\bar{\mu})=21$ phonon. The effect of the substantial purity of the M1 states is illustrated in the lower part of Fig. 5, showing the M1 strength distributions when only the $(\bar{\lambda}\bar{\mu})$ are included in the calculation. This is what is done in schematic approaches.[97] The spectrum so obtained is quite similar to the corresponding one deduced by including all core states.

The spectra of the reduced widths of ^{163}Dy, computed in the QPNM, are compared with the experimental data in Fig. 6. The following points are noteworthy: (i) The computed M1 transitions fall in the region of the observed peaks in all nuclei. The discrepancies in the energy distribution in relation to the experiments are of the same order as in the nearby doubly even nuclei. (ii) The $K^\pi\to K^\pi+1$ M1 transitions are fewer in number but in general much stronger than in the $K^\pi\to K^\pi-1$ case. As already said for ^{163}Dy, the M1 strength of the neighboring doubly even nuclei is shared equally by the two K_f^π states, but for $K_f^\pi=K_i^\pi-1$ the strength is further distributed, mostly among two out of the three J_f components of the K_f^π multiplet. (iii) The magnitude of the strongest M1 peaks is about twice the intensity of the corresponding observed transitions. In addition, the summed reduced widths are in general about twice the experimental values.

2. E1 transitions

In odd-mass nuclei the fragmentation mechanism of the $\Delta K=\pm 1$ E1 strength is obviously the same as for the M1 transitions. Exactly as in the case of the M1 transitions, the $\Delta K=1$ E1 strength is also shared equally by the $K_f^\pi=K_f^\pi-1$ and $K_f^\pi=K_f^\pi+1$ levels, and the $I_f^\pi=K_f^\pi$ states take 2/3 of the K_f^π strength. However, as in doubly even nuclei,[193] the $\Delta K=1$ E1 strength represents a small fraction of the total transition probability. This is concentrated mostly in the $\Delta K=0$ transitions. These transitions are in general more than five times stronger. As in the M1 case, the E1 states have a dominant configuration embodying the $(\bar{\lambda}\bar{\mu})$ phonon.

Figure 6 shows that the M1 widths are much larger than the corresponding $\Delta K=1$ E1 widths. Indeed, as in the doubly even nuclei, the E1 strength is concentrated almost entirely in the $\Delta K=0$ transitions. These can be quite strong. The strongest peaks are larger than the magnetic transitions and more than three times the experimental widths. These strong E1 transitions correspond to strong E1 excitations of collective octupole core states. However, no strong E1 transitions above 2 MeV have been observed in the nearby doubly even nuclei. One could reduce the strength of these transitions by using a smaller effective charge, as was done in Ref. 205. This new effective charge, however, would quench also the low-lying E1 transitions, thereby spoiling the agreement with experiment. This is still an unsolved problem, which requires detailed specific studies.

We can conclude that the occurrence of E1 transitions of appreciable strength in the observation region cannot be ruled out, but cannot be assessed with certainty because of the discrepancies between theory and experiment found in the doubly even nuclei for these transitions. On the other hand, the M1 and E1 transitions are predicted to carry different ΔK quantum numbers. More refined experiments may hopefully exploit this fact in order to settle upon the exact nature of the observed widths. In any case, the problem of reproducing the extreme fragmentation of the M1 strength, especially in some nuclei like ^{157}Gd, remains unsolved.

8. CONCLUSIONS

We have seen that the collective features of the low-lying M1 excitations, chiefly the quadratic deformation law, are described fairly well in several phenomenological approaches. All these models have been shown to be mutually correlated. They can actually be put within a unified context having the TRM as the common root. Each of them can indeed be converted into a TRM-like model when the variables which describe the shape oscillations of the nuclei are frozen. The differences among them are to be attributed mainly to the different microscopic structure underlying each model. While in fact the IBM boson operators are to be considered as highly correlated valence fermion pairs, in the other two interacting-boson models under investigation (NPD and GCSM) the bosons should be viewed, at least in lowest order, as highly correlated $p-h$ fermion states. The microscopic counterpart of the IBM is therefore the standard shell model, while the RPA is the microscopic scheme underlying the other boson models. We have shown that in their schematic version both the shell model and the RPA are intimately related to the TRM and actually provide the tools for computing the TRM quantities in a realistic way.

In going from schematic to realistic RPA descriptions, the correspondence with the TRM as well as with the other

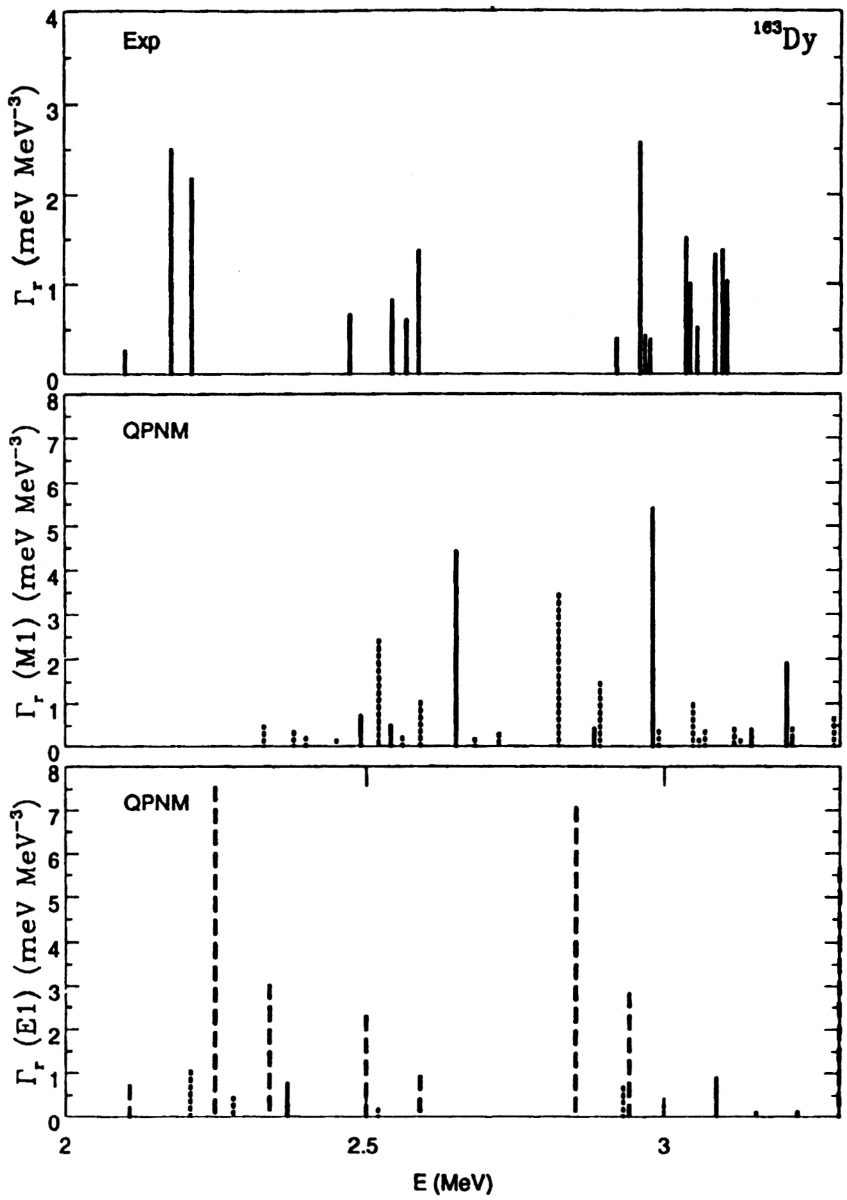

FIG. 6. Ground-state decay reduced-width distribution in ^{163}Dy. The full, dashed, and dotted lines refer, respectively, to $K_f=3/2$, 5/2, 7/2 final states.

phenomenological models is far from obvious. Because of the extreme fragmentation of the two-quasiparticle spectrum, the naive HO picture with a single degenerate $p-h$ level seems quite far from reality. It is rewarding that, because of the spin–spin interaction which pushes the spin excitations up in energy, the quadrupole pairing which rearranges the M1 strength distribution among different $p-h$ levels, and the recoil term, the fragmentation is drastically reduced.

The many RPA calculations carried out since the discovery of the mode have shown that such a mode is extremely sensitive to the choice of the s.p. energy and of the two-body interaction as well as to the approximations involved. Because of this extreme sensitivity, the calculations had to meet certain requirements. A major one was the removal of the redundant rotational mode from the physical M1 states. This problem has been clearly illustrated here, and a simple prescription for its solution has been given. All recent RPA calculations are free from this problem and tend toward converging results. Indeed, all of them agree in interpreting the low-lying M1 peaks around 3 MeV as the signature of a scissors-like rotational oscillation between proton and neutron deformed fluids. The simple TRM picture therefore appears valid. However, one should think of a rotational oscillation between two superfluids rather than two rigid bodies or two normal irrotational fluids.

The only point which is still under debate is the collective character of the mode. We observe in this respect that the collectivity of this M1 excitation should not be "measured" in terms of s.p. units as, for instance, in the case of the E1 or E2 giant resonances. The mode under study here arises in fact from deformation and disappears as the deformation is switched off. This emerges nicely from the δ^2 dependence of the M1 strength. A more sensitive test of the collectivity of the mode is provided by the M1 energy-weighted sum rule. Recent calculations[185] show that the observed strength falls short of exhausting such a sum rule. A strong indication in this respect is further provided by the fact that the excitation is observed throughout all deformed (light and heavy) nuclei and that its strength varies smoothly with the deformation.

The RPA descriptions are not able to reproduce faithfully the M1 energy spectrum. Progress in this direction has been achieved by going beyond the RPA. This has been done by allowing for the coupling to the two-phonon RPA state within the QPNM. Even this extension seems insufficient. It should be pointed out, however, that the calculations carried out in this context are parameter-free. Minor adjustments may greatly improve the agreement with experiment.

One of the most exciting recent discoveries was the detection of M1 excitations exhibiting the properties of the scissors mode in odd-mass nuclei but with a much more fragmented strength. The only thorough microscopic description of these spectra has been carried out recently in the QPNM. Many aspects have been clarified. Many problems remain unsettled. The calculation in fact indicates that the occurrence of E1 excitations intermixed with M1 transitions cannot be ruled out. It also indicates that the detected total strength is considerably smaller than what is produced by the calculations. Moreover, the extreme fragmentation observed in some nuclei remains an unexplained puzzle.

Let us now consider future prospects. There is great interest in the possible occurrence of a high-energy mode of scissors nature. The sharing of the M1 strength among a low- and a high-energy mode is reminiscent of the isoscalar E2 strength known to be concentrated in a high- and a low-energy mode. The detection of such a mode is related to the discovery of the E2 isovector giant resonance in deformed nuclei.

Strongly excited M1 excitations of scissors nature, both at low and at high energy, are predicted also for superdeformed nuclei. Whether these modes can be observed directly is an open question.

The prospect of finding the mode in γ-soft nuclei is becoming a reality. Pursuit of the search for M3 transitions would help to complete the picture.

We would like to conclude by saying that the occurrence of orbital M1 excitations has uncovered a beautiful example of dynamical symmetry in nuclei and has provided a unique and sensitive testing ground for many phenomenological models as well as for microscopic theories. From its extensive study we have tested effective interactions and correlations among nucleons in nuclei, and we have enriched considerably our knowledge about the low-energy nuclear properties.

[1]D. Bohle, A. Richter, W. Steffen, A. E. L. Dieperink, N. Lo Indice, F. Palumbo, and O. Scholten, Phys. Lett. B**137**, 27 (1984).

[2]N. Lo Iudice and F. Palumbo, Phys. Rev. Lett. **41**, 1532 (1978); G. De Franceschi, F. Palumbo, and N. Lo Iudice, Phys. Rev. C **29**, 1496 (1984).

[3]F. Iachello, Nucl. Phys. A **358**, 89c (1981).

[4]A. E. L. Dieperink, Prog. Part. Nucl. Phys. **9**, 121 (1983).

[5]R. R. Hilton, Z. Phys. A **316**, 121 (1984).

[6]A. Richter, Nucl. Phys. A **507**, 99c (1990); **522**, 139c (1991); **553**, 417c (1991).

[7]P. von Brentano, A. Zilges, R. D. Heil, R.-D. Herzberg, U. Kneissl, H. H. Pitz, and C. Wesselborg, Nucl. Phys. A **557**, 593c (1993).

[8]A. Richter, Prog. Part. Nucl. Phys. **34**, 261 (1995).

[9]U. Kneissl, J. Margraf, H. H. Pitz, P. von Brentano, R.-D. Herzberg, and A. Zilges, Prog. Part. Nucl. Phys. **34**, 285 (1995).

[10]U. Kneissl, H. H. Pitz, and A. Zilges, Prog. Part. Nucl. Phys. **37**, 349 (1996).

[11]W. Ziegler, C. Rangacharyulu, A. Richter, and C. Spieler, Phys. Rev. Lett. **65**, 2515 (1990).

[12]C. Rangacharyulu, A. Richter, H. J. Wörtche, W. Ziegler, and R. F. Casten, Phys. Rev. C **43**, R949 (1991).

[13]J. Margraf, R. D. Heil, U. Kneissl, U. Maier, H. H. Pitz, H. Friedrichs, S. Lindenstruth, B. Schlitt, C. Wesselborg, P. von Brentano, R.-D. Herzberg, and A. Zilges, Phys. Rev. C **47**, 1474 (1993).

[14]P. von Brentano, A. Zilges, R.-D. Herzberg, U. Kneissl, J. Margraf, and H. H. Pitz, Nucl. Phys. A **577**, 191c (1994) and references therein.

[15]N. Pietralla, P. von Brentano, R.-D. Herzberg, A. Zilges, U. Kneissl, J. Margraf, H. Maser, and H. H. Pitz, Phys. Rev. C **52**, R2317 (1995).

[16]R. D. Heil, B. Kasten, W. Scharfe, P. A. Butler, H. Friedrichs, S. D. Hoblit, U. Kneissl, S. Lindenstruth, M. Ludwig, G. Müller, H. H. Pitz, K. W. Rose, M. Schumacher, U. Seemann, J. Simpson, P. von Brentano, Th. Weber, C. Wesselborg, and A. Zilges, Nucl. Phys. A **506**, 223 (1990).

[17]H. Friedrichs, B. Schlitt, J. Margraf, S. Lindenstruth, C. Wesselborg, R. D. Heil, H. H. Pitz, U. Kneissl, P. von Brentano, R.-D. Herzberg, A. Zilges, D. Häger, G. Müller, and M. Schumacher, Phys. Rev. C **45**, R892 (1992).

[18]A. Zilges, P. von Brentano, H. Friedrichs, R. D. Heil, U. Kneissl, S. Lindenstruth, H. H. Pitz, and C. Wesselborg, Z. Phys. A **340**, 155 (1991).

[19]H. Friedrichs, D. Häger, P. von Brentano, R. D. Heil, R.-D. Herzberg, U. Kneissl, J. Margraf, G. Müller, H. H. Pitz, B. Schlitt, M. Schumacher, C. Wesselborg, and A. Zilges, Nucl. Phys. A **567**, 266 (1994).

[20]J. Margraf, T. Eckert, M. Rittner, I. Bauske, O. Beck, U. Kneissl, H. Maser, H. H. Pitz, A. Schiller, P. von Brentano, R. Fischer, R.-D. Herzberg, N. Pietralla, A. Zilges, and H. Friedrichs, Phys. Rev. C **52**, 2429 (1995).

[21]D. Frekers, H. J. Wörtche, A. Richter, A. Abegg, R. E. Azuma, A. Celler, C. Chan, T. E. Drake, K. P. Jackson, J. D. King, C. A. Miller, R. Schubank, M. C. Vetterli, and S. Yen, Phys. Lett. B **244**, 178 (1990).

[22]A. Richter, Nucl. Phys. A **553**, 417c (1993).

[23]P. Van Isacker, K. Heyde, M. Waroquier, J. Moreau, and O. Scholten, Phys. Lett. B**144**, 1 (1984).

[24]O. Scholten, A. E. L. Dieperink, K. Heyde, and P. Van Isacker, Phys. Lett. B **149**, 279 (1984).

[25]S. Pittel, J. Dukelsky, R. P. J. Perazzo, and H. M. Sofia, Phys. Lett. B **144**, 145 (1984).

[26]T. Otsuka and J. N. Ginocchio, Phys. Rev. Lett. **54**, 777 (1985).

[27]O. Scholten, K. Heyde, P. Van Isacker, J. Jolie, J. Moreau, and M. Waroquier, Nucl. Phys. A **438**, 41 (1985).

[28]B. R. Barrett and P. Halse, Phys. Lett. B **155**, 133 (1985).

[29]P. Van Isacker, K. Heyde, J. Jolie, and A. Sevrin, Ann. Phys. (N.Y.) **171**, 253 (1986) and references therein.

[30]A. Faessler, R. Nojarov, Phys. Lett. B **166**, 367 (1986); R. Nojarov, Z. Bochnacki, and A. Faessler, Z. Phys. A **324**, 289 (1986); A. Faessler, Z. Bochnacki, and R. Nojarov, J. Phys. G **12**, L47 (1986).

[31]S. G. Rohozinski and W. Greiner, Z. Phys. A **322**, 271 (1985).

[32]A. A. Raduta, A. Faessler, and V. Ceasescu, Phys. Rev. C **36**, 2111 (1987).

[33]A. A. Raduta, I. I. Ursu, and D. S. Delion, Nucl. Phys. A **475**, 439 (1987).

[34]E. Lipparini and S. Stringari, Phys. Lett. B **130**, 139 (1983).

[35]T. Suzuki and D. J. Rowe, Nucl. Phys. A **289**, 461 (1977).

[36]D. R. Bes and R. A. Broglia, Phys. Lett. B **137**, 141 (1984).

[37]H. Kurasawa and T. Suzuki, Phys. Lett. B **144**, 151 (1984).

[38]A. E. L. Dieperink and E. Moya de Guerra, Phys. Lett. B **189**, 267 (1987).

[39]L. Zamick, Phys. Rev. C **31**, 1955 (1985); Phys. Lett. B **167**, 1 (1986); Phys. Rev. C **33**, 691 (1986).

[40]H. Liu and L. Zamick, Phys. Rev. C **36**, 2057, 2064 (1987); Nucl. Phys. A **467**, 29 (1987).

[41]B. Castel and L. Zamick, Phys. Rep. **148**, 217 (1987).

[42]L. Zamick and D. C. Zheng, Phys. Rev. C **44**, 2522 (1991); **46**, 2106 (1992).

[43]M. Abdelaziz, M. J. Thompson, J. P. Elliot, and J. A. Evans, J. Phys. G **14**, 219 (1988).

[44]M. Abdelaziz, M. J. Thompson, J. P. Elliot, and J. A. Evans, Nucl. Phys. A **503**, 452 (1989).

[45]L. Chaves and A. Poves, Phys. Rev. C **34**, 1137 (1986).

[46]A. Poves, J. Retamosa, and E. Moya de Guerra, Phys. Rev. C **39**, 1356 (1989).

[47]J. Retamosa, J. M. Udias, A. Poves, and E. Moya de Guerra, Nucl. Phys. A **511**, 221 (1990).
[48]O. Castaños, J. P. Draayer, and Y. Leschber, Nucl. Phys. A **473**, 494 (1987).
[49]O. Castaños, J. P. Draayer, and Y. Leschber, Ann. Phys. (N.Y.) **180**, 290 (1987).
[50]E. Hammaren, K. W. Schmid, A. Faessler, and F. Grümmer, Phys. Lett. B **171**, 347 (1986).
[51]E. Hammaren, P. Heikkinen, K. W. Schmid, and A. Faessler, Nucl. Phys. A **541**, 226 (1992).
[52]S. Iwasaki and K. Hara, Phys. Lett. B **144**, 9 (1984).
[53]I. Hamamoto and S. Åberg, Phys. Lett. B **145**, 163 (1984).
[54]I. Hamamoto and S. Åberg, Phys. Scr. **34**, 697 (1986).
[55]R. R. Hilton, S. Iwasaki, H. J. Mang, P. Ring, and M. Faber, in *Microscopic Approaches to Nuclear Structure Calculations*, edited by A. Covello (Editrice Compositori Bologna, 1986), p. 357.
[56]I. Hamamoto and C. Rönstrom, Phys. Lett. B **194**, 6 (1987).
[57]O. Civitarese, A. Faessler, and R. Nojarov, Phys. Rev. C **35**, 2310 (1987).
[58]R. Nojarov, A. Faessler, and O. Civitarese, Phys. Lett. B **183**, 122 (1987).
[59]J. Speth and D. Zawischa, Phys. Lett. B **211**, 247 (1988); **219**, 229 (1989).
[60]R. Nojarov and A. Faessler, Nucl. Phys. A **484**, 1 (1988).
[61]K. Sugawara-Tanabe and A. Arima, Phys. Lett. B **206**, 573 (1988).
[62]F. G. Scholtz, R. Nojarov, and A. Faessler, Phys. Rev. Lett. **63**, 1356 (1989).
[63]A. Faessler and R. Nojarov, Phys. Rev. C **41**, 1243 (1990).
[64]R. Nojarov and A. Faessler, Z. Phys. A **336**, 151 (1990).
[65]A. Faessler, R. Nojarov, and F. G. Scholtz, Nucl. Phys. A **515**, 237 (1990).
[66]A. Faessler, D. T. Khoa, M. Grigorescu, and R. Nojarov, Phys. Rev. Lett. **65**, 2978 (1990).
[67]D. Zawischa, M. Macfarlane, and J. Speth, Phys. Rev. C **42**, 1461 (1990).
[68]D. Zawischa and J. Speth, Phys. Lett. B**252**, 4 (1990).
[69]I. Hamamoto and C. Magnusson, Phys. Lett. B **260**, 6 (1991).
[70]C. Magnusson, Phys. Scr. **43**, 460 (1991).
[71]R. Nojarov, A. Faessler, and P. O. Lipas, Nucl. Phys. A **533**, 381 (1991); **537**, 707 (1992).
[72]I. Hamamoto and W. Nazarewicz, Phys. Lett. B **297**, 25 (1992).
[73]R. Nojarov, A. Faessler, P. Sarriguren, E. Moya de Guerra, and M. Grigorescu, Nucl. Phys. A **563**, 349 (1993).
[74]P. Sarriguren, E. Moya de Guerra, R. Nojarov, and A. Faessler, J. Phys. G **19**, 291 (1993); **20**, 315 (1994).
[75]R. Nojarov and A. Faessler, Nucl. Phys. A **572**, 17 (1994).
[76]R. Nojarov, A. Faessler, and M. Dingfelder, Phys. Rev. C **51**, 2449 (1995).
[77]A. A. Raduta, N. Lo Iudice, and I. I. Ursu, Nucl. Phys. A **584**, 84 (1995).
[78]C. De Coster and K. Heyde, Nucl. Phys. A **529**, 507 (1991).
[79]K. Heyde and C. De Coster, Phys. Rev. C **44**, R2262 (1991).
[80]E. Garrido, E. Moya de Guerra, P. Sarriguren, and J. M. Udias, Phys. Rev. C **44**, R1250 (1991).
[81]E. Moya de Guerra and L. Zamick, Phys. Rev. C **47**, 2604 (1993).
[82]R. R. Hilton, W. Höhenberger, and H. J. Mang, Phys. Rev. C **47**, 602 (1993).
[83]B. H. Smith, X. W. Pan, D. H. Feng, and M. Guidry, Phys. Rev. Lett. **75**, 3086 (1995).
[84]J. N. Ginocchio, Phys. Lett. B **265**, 6 (1991).
[85]T. Mizusaki, T. Otsuka, and M. Sugita, Phys. Rev. C **44**, R1277 (1991).
[86]K. Heyde, C. De Coster, A. Richter, and H.-J. Wörtche, Nucl. Phys. A **549**, 103 (1992).
[87]K. Heyde, C. De Coster, D. Ooms, and A. Richter, Phys. Lett. B **312**, 267 (1993).
[88]K. Heyde, C. De Coster, and D. Ooms, Phys. Rev. C **49**, 156 (1994).
[89]N. Lo Iudice, A. A. Raduta, and D. S. Delion, Phys. Lett. B **300**, 195 (1993); Phys. Rev. C **50**, 127 (1994).
[90]N. Lo Iudice and A. Richter, Phys. Lett. B **304**, 193 (1993).
[91]P. von Neumann-Cosel, J. N. Ginocchio, H. Bauer, and A. Richter, Phys. Rev. Lett. **75**, 4178 (1995).
[92]N. Lo Iudice, Phys. Rev. C **53**, 2171 (1996).
[93]V. G. Soloviev, A. V. Sushkov, N. Yu. Shirikova, and N. Lo Iudice, Nucl. Phys. A **600**, 155 (1996).
[94]V. G. Soloviev, *Theory of Atomic Nuclei: Quasiparticles and Phonons* (Institute of Physics, Philadelphia, 1992).
[95]P. Van Isacker and A. Frank, Phys. Lett. B **225**, 1 (1989).
[96]A. Frank, J. M. Arias, and P. Van Isacker, Nucl. Phys. A **531**, 125 (1991).
[97]A. A. Raduta and N. Lo Iudice, Z. Phys. A **334**, 403 (1989).
[98]A. A. Raduta and D. S. Delion, Nucl. Phys. A **513**, 11 (1990).
[99]N. Huxel, W. Ahner, H. Diesener, P. Von Neumann-Cosel, C. Rangacharyulu, A. Richter, C. Spieler, W. Ziegler, C. De Coster, and K. Heyde, Nucl. Phys. A **539**, 478 (1992).
[100]I. Bauske, J. M. Arias, P. von Brentano, A. Frank, H. Friedrichs, R. D. Heil, R. D. Herzberg, F. Hoyler, P. Van Isacker, U. Kneissl, J. Margraf, H. H. Pitz, C. Wesselborg, and A. Zilges, Phys. Rev. Lett. **71**, 975 (1993).
[101]C. Schlegel, P. von Neumann-Cosel, A. Richter, and P. van Isacker, Phys. Lett. B **375**, 21 (1996).
[102]V. G. Soloviev, A. V. Sushkov, and N. Yu. Shirikova, Phys. Rev. C **53**, 1022 (1996).
[103]V. G. Soloviev, A. V. Sushkov, N. Yu. Shirikova, and N. Lo Iudice, Nucl. Phys. A **613**, 1 (1997).
[104]M. Goldhaber and E. Teller, Phys. Rev. **73**, 1156 (1948).
[105]H. Steinwedel and J. H. D. Jensen, Z. Naturforsch. 5a, 413 (1950).
[106]N. Lo Iudice, Phys. Rev. C **34**, 1501 (1986).
[107]D. Bohle, G. Kilgus, A. Richter, C. W. de Jager, and H. de Vries, Phys. Lett. B**195**, 326 (1987).
[108]A. Richter, in *Contemporary Topics in Nuclear Structure Physics*, edited by R. F. Casten, A. Frank, M. Moshinsky, and S. Pittel (World Scientific, Singapore, 1988), p. 127.
[109]U. E. P. Berg, C. Bläsing, J. Drexler, R. D. Heil, U. Kneissel, W. Naatz, R. Ratzek, S. Schennach, R. Stock, T. Weber, H. Wickert, B. Fischer, H. Hollick, and D. Kollewe, Phys. Lett. B **149**, 59 (1984).
[110]G. Alaga, K. Alder, A. Bohr, and B. R. Mottelson, K. Dan. Vidensk. Selsk. Mat. Fys. Medd. **29**, 1 (1955).
[111]D. Bohle, G. Küchler, A. Richter, and W. Steffen, Phys. Lett. B **148**, 260 (1984).
[112]C. Wesselborg, P. von Brentano, K. O. Zell, R. D. Heil, H. H. Pitz, V. E. P. Berg, U. Kneissl, S. Lindenstruth, U. Seemann, and R. Stock, Phys. Lett. B **207**, 22 (1988).
[113]U. Hartmann, D. Bohle, F. Humbert, and A. Richter, Nucl. Phys. A **499**, 93 (1989).
[114]H. H. Pitz, U. E. P. Berg, R. D. Heil, U. Kneissl, R. Stock, C. Wesselborg, and P. von Brentano, Nucl. Phys. A **492**, 411 (1989).
[115]B. Kasten, R. D. Heil, P. von Brentano, P. A. Butler, S. D. Hoblit, U. Kneissl, S. Lindenstruth, G. Müller, H. H. Pitz, K. W. Rose, W. Scharfe, M. Schumacher, U. Seemann, Th. Weber, C. Wesselborg, and A. Zilges, Phys. Rev. Lett. **63**, 609 (1989).
[116]H. H. Pitz, R. D. Heil, U. Kneissl, S. Lindenstruth, U. Seemann, C. Wesselborg, A. Zilges, P. von Brentano, S. D. Hoblit, and A. M. Nathan, Nucl. Phys. A **509**, 587 (1990).
[117]A. Zilges, P. von Brentano, C. Wesselborg, R. D. Heil, U. Kneissl, S. Lindenstruth, H. H. Pitz, U. Seemann, and R. Stock, Nucl. Phys. A **507**, 399 (1990).
[118]R.-D. Herzberg, A. Zilges, P. von Brentano, R. D. Heil, U. Kneissl, J. Margraf, H. H. Pitz, H. Friedrichs, S. Lindenstruth, and C. Wesselborg, Nucl. Phys. A **563**, 445 (1993).
[119]M. Maser, S. Lindenstruth, I. Bauske, O. Beck, P. von Brentano, T. Eckert, H. Friedrichs, R. D. Heil, R. D. Herzberg, A. Jung, U. Kneissl, J. Margraf, N. Pietralla, H. H. Pitz, C. Wesselborg, and A. Zilges, Phys. Rev. C **53**, 2749 (1996).
[120]C. Djalali, N. Marty, M. Morlet, A. Willis, J. C. Jourdain, D. Bohle, U. Hartman, G. Küchler, A. Richter, G. Caskey, G. M. Crawley, and A. Galonsky, Phys. Lett. B **164**, 269 (1985).
[121]A. Richter, Prog. Part. Nucl. Phys. **13**, 1 (1985).
[122]A. Degener, C. Bläsing, R. D. Heil, A. Jung, U. Kneissl, H. H. Pitz, H. Schacht, S. Schennach, R. Stock, and C. Wesselborg, Nucl. Phys. A **513**, 29 (1990).
[123]R. D. Heil, H. H. Pitz, V. E. P. Berg, U. Kneissl, K. D. Hummel, G. Kilgus, D. Bohle, A. Richter, C. Wesselborg, and P. von Brentano, Nucl. Phys. A **476**, 39 (1988).
[124]J. Margraf, A. Degener, H. Friedrichs, R. D. Heil, A. Jung, U. Kneissl, S. Lindenstruth, H. H. Pitz, H. Schacht, U. Seemann, R. Stock, C. Wesselborg, A. Zilges, and P. von Brentano, Phys. Rev. C **42**, 771 (1990).
[125]C. Wesselborg, K. Schiffer, K. O. Zell, P. von Brentano, D. Bohle, A. Richter, G. P. A. Berg, B. Brinkmöller, J. G. M. Römer, F. Osterfeld, and M. Yabe, Z. Phys. A **323**, 485 (1986).
[126]D. Frekers, D. Bohle, A. Richter, A. Abegg, R. E. Azuma, A. Celler, C. Chan, T. E. Drake, K. P. Jackson, J. D. King, C. A. Miller, R. Schubank, J. Watson, and S. Yen, Phys. Lett. B **218**, 439 (1989).
[127]D. Bohle, A. Richter, U. E. P. Berg, J. Drexler, R. D. Heil, U. Kneissl,

H. Metzger, R. Stock, B. Fischer, H. Hollick, and D. Kollewe, Nucl. Phys. A **458**, 205 (1986).
[128]S. J. Freeman, R. Chapman, J. L. Durell, M. A. C. Hotchkis, F. Khazaie, J. C. Lisle, J. N. Mo, A. M. Bruce, R. A. Cunningham, P. V. Drumm, D. D. Warner, and J. D. Garrett, Phys. Lett. B **222**, 347 (1988).
[129]S. J. Freeman, R. Chapman, J. L. Durell, M. A. C. Hotchkis, F. Khazaie, J. C. Lisle, and J. N. Mo, Nucl. Phys. A **554**, 333 (1993).
[130]J. Margraf, C. Wesselborg, R. D. Heil, U. Kneissl, H. H. Pitz, C. Rangacharyulu, A. Richter, H. J. Wörtche, and W. Ziegler, Phys. Rev. C **45**, R521 (1992).
[131]P. von Brentano, J. Eberth, J. Enders, L. Esser, R.-D. Herzberg, N. Huxel, H. Meise, P. von Neumann-Cosel, N. Nicolay, M. Maser, N. Pietralla, H. Prade, J. Reif, A. Richter, C. Schlegel, R. Schwengner, S. Skoda, H. G. Thomas, I. Wiedenhöver, G. Winter, and A. Zilges, Phys. Rev. Lett. **76**, 2029 (1996).
[132]M. Maser, N. Pietralla, P. von Brentano, R. D. Herzberg, U. Kneissl, J. Margraf, H. H. Pitz, and A. Zilges, Phys. Rev. C **54**, 1 (1996).
[133]A. Bohr and B. R. Mottelson, *Nuclear Structure* (Benjamin, New York, 1975), Vol. 2, Chap. 6.
[134]N. Lo Iudice, in *Capture Gamma-Ray Spectroscopy*, edited by J. Berg (World Scientific, Singapore, 1994), p. 154.
[135]F. Palumbo and A. Richter, Phys. Lett. B **158**, 101 (1985).
[136]N. Lo Iudice, E. Lipparini, S. Stringari, F. Palumbo, and A. Richter, Phys. Lett. B **161**, 18 (1985).
[137]R. Nojarov, Nucl. Phys. A **571**, 93 (1994).
[138]A. Faessler, Nucl. Phys. **85**, 653 (1966).
[139]S. G. Rohozinski, D. Troltenier, J. A. Maruhn, and W. Greiner, Z. Phys. A **330**, 23 (1988).
[140]A. A. Raduta, V. Ceasescu, A. Gheorghe, and R. M. Dreizler, Phys. Lett. B **99**, 444 (1981); Nucl. Phys. A **381**, 253 (1982).
[141]A. A. Raduta and D. S. Delion, Nucl. Phys. A **491**, 24 (1989).
[142]D. Bohle, A. Richter, C. W. de Jager, and H. de Vries, Z. Phys. A **328**, 463 (1987).
[143]A. A. Raduta, I. I. Ursu, and A. Faessler, Nucl. Phys. A **489**, 20 (1988).
[144]A. Arima and F. Iachello, Phys. Rev. Lett. **35**, 1069 (1975); Ann. Phys. (N.Y.) **99**, 253 (1976); **111**, 201 (1978); **123**, 468 (1979).
[145]For a review, see A. Arima and F. Iachello, Adv. Nucl. Phys. **13**, 139 (1984).
[146]A. Arima, T. Otsuka, F. Iachello, and I. Talmi, Phys. Lett. B **66**, 205 (1977); T. Otsuka, A. Arima, F. Iachello, and I. Talmi, Phys. Lett. B **76**, 139 (1978).
[147]M. Sambataro and A. E. L. Dieperink, Phys. Lett. B **107**, 249 (1981).
[148]M. Sambataro, O. Scholten, A. E. L. Dieperink, and G. Piccitto, Nucl. Phys. A **423**, 333 (1984).
[149]A. Wolf, R. F. Casten, and D. D. Warner, Phys. Lett. B **190**, 19 (1987).
[150]A. Wolf, O. Scholten, and R. F. Casten, Phys. Lett. B **312**, 372 (1993).
[151]P. O. Lipas, M. Koskinen, H. Harter, R. Nojarov, and A. Faessler, Phys. Lett. B **230**, 1 (1989); Nucl. Phys. A **509**, 509 (1990).
[152]P. O. Lipas, H. Harter, R. Nojarov, A. Faessler, and M. Koskinen, J. Phys. G **17**, 971 (1991).
[153]R. F. Casten, D. S. Brenner, and P. E. Haustein, Phys. Rev. Lett. **58**, 658 (1987).
[154]See, for instance, N. R. Walet, P. I. Brussard, and A. E. L. Dieperink, Phys. Lett. B **63**, 1 (1985).
[155]A. B. Balantekin and B. R. Barrett, Phys. Rev. C **32**, 288 (1985); **33**, 1842 (1986).
[156]R. Bijker, Phys. Rev. C **32**, 1442 (1985).
[157]S. Pittel and J. Dukelsky, Phys. Rev. C **32**, 335 (1985).
[158]N. Lo Iudice, F. Palumbo, A. Richter, and H. Wörtche, Phys. Rev. C **42**, 241 (1990).
[159]O. Scholten, K. Heyde, and P. Van Isacker, Phys. Rev. Lett. **55**, 1866 (1985).
[160]K. Heyde and J. Sau, Phys. Rev. C **30**, 1355 (1984).
[161]T. Oda, M. Hino, and K. Muto, Phys. Lett. B **190**, 14 (1987).
[162]M. Hino, K. Muto, and T. Oda, J. Phys. G **13**, 1119 (1987).
[163]J. P. Elliott, Proc. R. Soc. London, Ser. A **245**, 128, 562 (1958).
[164]A. Arima, M. Harvey, and K. Shimizu, Phys. Lett. B **30**, 517 (1969).
[165]K. T. Hecht and A. Adler, Nucl. Phys. A **137**, 129 (1969).
[166]D. Braunschweig and K. T. Hecht, Phys. Lett. B **77**, 33 (1978).
[167]J. P. Draayer and K. J. Weeks, Phys. Rev. Lett. **16**, 1422 (1983).
[168]J. P. Draayer and K. J. Weeks, Ann. Phys. (N.Y.) **156**, 41 (1984).
[169]D. J. Rowe, *Nuclear Collective Motion* (Methuen, London, 1970).
[170]V. G. Soloviev, *Theory of Complex Nuclei* (Pergamon Press, Oxford, 1976).
[171]N. Lo Iudice, Phys. Rev. C **38**, 2895 (1988).
[172]C. De Coster and K. Heyde, Phys. Rev. Lett. **63**, 2797 (1989).
[173]C. De Coster and K. Heyde, Nucl. Phys. A **524**, 441 (1991).
[174]T. Shimano and A. Ikeda, Prog. Theor. Phys. **88**, 599 (1992).
[175]A. Ikeda and T. Shimano, Nucl. Phys. A **557**, 573c (1993).
[176]K. Heyde and C. De Coster, Phys. Lett. B **305**, 322 (1993).
[177]N. Lo Iudice and A. Richter, Phys. Lett. B **228**, 291 (1989).
[178]M. I. Baznat and N. I. Pyatov, Sov. J. Nucl. Phys. **21**, 365 (1975).
[179]N. Lo Iudice, Nucl. Phys. A **605**, 61 (1996).
[180]T. Kishimoto, J. M. Moss, D. H. Youngblood, J. D. Bronson, C. M. Rozsa, D. R. Brown, and A. D. Bacher, Phys. Rev. Lett. **35**, 552 (1975).
[181]H. Sakamoto and T. Kishimoto, Nucl. Phys. A **501**, 205 (1989).
[182]S. Åberg, Phys. Lett. B **157**, 9 (1985).
[183]S. Åberg, Nucl. Phys. A **473**, 1 (1987).
[184]M. S. Fayache, S. Shelly Sharma, and L. Zamick, Phys. Lett. B **357**, 1 (1995).
[185]N. Lo Iudice, submitted to Nucl. Phys. A.
[186]A. Faessler, in *New Perspeclives in Nuclear Structure*, edited by A. Covello (World Scientific, Singapore, 1996).
[187]C. De Coster and K. Heyde, Phys. Rev. Lett. **66**, 2456 (1991).
[188]C. De Coster, K. Heyde, and A. Richter, Nucl. Phys. A **542**, 375 (1992).
[189]V. G. Soloviev, A. V. Sushkov, and N. Yu. Shirikova, Sov. J. Nucl. Phys. **53**, 65 (1991); **54**, 748 (1991).
[190]V. G. Soloviev and A. V. Sushkov, Phys. Lett. B **262**, 189 (1991).
[191]V. G. Soloviev and N. Yu. Shirikova, Nucl. Phys. A **542**, 410 (1992).
[192]V. G. Soloviev, A. V. Sushkov, and N. Yu. Shirikova, Phys. Part. Nucl. **25**, 157 (1994).
[193]V. G. Soloviev and A. V. Sushkov, Phys. At. Nucl. **57**, 1304 (1994).
[194]V. G. Soloviev, A. V. Sushkov, and N. Yu. Shirikova, Nucl. Phys. A **568** 244 (1994); Int. J. Mod. Phys. E **3**, 1227 (1994).
[195]V. G. Soloviev, A. V. Sushkov, and N. Yu. Shirikova, Phys. Rev. C **51**, 551 (1995); Yad. Fiz. **59**, 57 (1996) [Phys. At. Nucl. **59**, 51 (1996)].
[196]J. Berzins, P. Prokofjevs, R. Georgii, T. Hucke, T. von Egidy, G. Hlawatsch, J. Klora, V. G. Soloviev, A. V. Sushkov, and N. Yu. Shirikova, Nucl. Phys. A **584**, 413 (1995).
[197]F. A. Gareev, S. P. Ivanova, V. G. Soloviev, and S. I. Fedotov, Sov. J. Part. Nucl. **4**, 357 (1973).
[198]V. G. Soloviev, Z. Phys. A **334**, 143 (1989).
[199]G. J. Gallagher and S. A. Moszkowski, Phys. Rev. **111**, 1282 (1958).
[200]E. Lipparini and A. Richter, Phys. Lett. B **144**, 13 (1984).
[201]V. G. Soloviev, Phys. Lett. **16**, 308 (1965).
[202]V. G. Soloviev, V. O. Nesterenko, and S. I. Bastrukov, Z. Phys. A **309**, 353 (1983).
[203]V. G. Soloviev, A. V. Sushkov, and N. Yu. Shirikova, J. Phys. G **21**, 1217 (1995).
[204]V. G. Soloviev, Yad. Fiz. **40**, 1163 (1984) [Sov. J. Nucl. Phys. **40**, 740 (1984)].
[205]See, for instance, I. Hamamoto, Nucl. Phys. A **205**, 225 (1973); **557**, 515c (1993).

This article was published in English in the original Russian journal. It is reproduced here with the stylistic changes by the Translations Editor.